Possible Aerosol Effects on Lightning Activity and Structure of Hurricanes

A. KHAIN, N. COHEN, B. LYNN, AND A. POKROVSKY

Department of Atmospheric Sciences, The Hebrew University of Jerusalem, Jerusalem, Israel

(Manuscript received 14 November 2007, in final form 17 April 2008)

ABSTRACT

According to observations of hurricanes located relatively close to the land, intense and persistent lightning takes place within a 250–300-km radius ring around the hurricane center, whereas the lightning activity in the eyewall takes place only during comparatively short periods usually attributed to eyewall replacement. The mechanism responsible for the formation of the maximum flash density at the tropical cyclone (TC) periphery is not well understood as yet. In this study it is hypothesized that lightning at the TC periphery arises under the influence of small continental aerosol particles (APs), which affect the microphysics and the dynamics of clouds at the TC periphery. To show that aerosols change the cloud microstructure and the dynamics to foster lightning formation, the authors use a 2D mixed-phase cloud model with spectral microphysics. It is shown that aerosols that penetrate the cloud base of maritime clouds dramatically increase the amount of supercooled water, as well as the ice contents and vertical velocities. As a result, in clouds developing in the air with high AP concentration, ice crystals, graupel, frozen drops and/or hail, and supercooled water can coexist within a single cloud zone, which allows collisions and charge separation. The simulation of possible aerosol effects on the landfalling tropical cyclone has been carried out using a 3-km-resolution Weather Research and Forecast (WRF) mesoscale model. It is shown that aerosols change the cloud microstructure in a way that permits the attribution of the observed lightning structure to the effects of continental aerosols. It is also shown that aerosols, which invigorate clouds at 250–300 km from the TC center, decrease the convection intensity in the TC center, leading to some TC weakening. The results suggest that aerosols change the intensity and the spatial distribution of precipitation in landfalling TCs and can possibly contribute to the weekly cycle of the intensity and precipitation of landfalling TCs. More detailed investigations of the TC–aerosol interaction are required.

1. Introduction

Tropical cyclones (TCs) are known for their destructive power, particularly as they make landfall. TCs are often accompanied by extreme winds, storm surges, and torrential rainfall. The TC wind fields, the area of heavy rain, and the rain rate are determined by cloud microphysical processes. At the same time, both experimental and numerical investigations of cloud microphysics in TCs are quite limited. Microphysical observations are usually limited by the zones of the melting level (McFarquhar and Black 2004). Lightning is one of the factors that can shed light on the microphysical cloud structure and the TC evolution. For instance, increasing lightning indicates the invigoration of convection together with increasingly larger volumes of graupel or small hail/frozen drops aloft, which strengthen updrafts and increase the probability of heavier rainfall (e.g., Lhermitte and Krehbiel 1979; Wiens et al. 2005; Fierro et al. 2007, hereafter FL07). The presence of lightning activity in storms crossing the West African coast can be a precursor to TC formation (Chronis et al. 2007). The appearance and intensification of lightning in the eyewall can be a predictor of TC intensification (Orville and Coyne 1999; Molinari et al. 1999, hereafter MMI99; Shao et al. 2005; Demetriades and Holle 2006; FL07). Rodgers et al. (2000) found that the closer the lightning is to the storm center, the more likely the TC is to intensify. The latter makes lightning and its distribution in TCs an important characteristic that can serve as a predictor of TC intensity and precipitation changes.

Molinari et al. (1994, 1999) analyzed the radial distribution of lightning in hurricanes approaching the United States coast using the National Lightning Detection Network data. This system detects only the

Corresponding author address: Prof. Alexander Khain, The Hebrew University of Jerusalem, Givat Ram, Jerusalem 91907, Israel.
E-mail: khain@vms.huji.ac.il

DOI: 10.1175/2008JAS2678.1

© 2008 American Meteorological Society

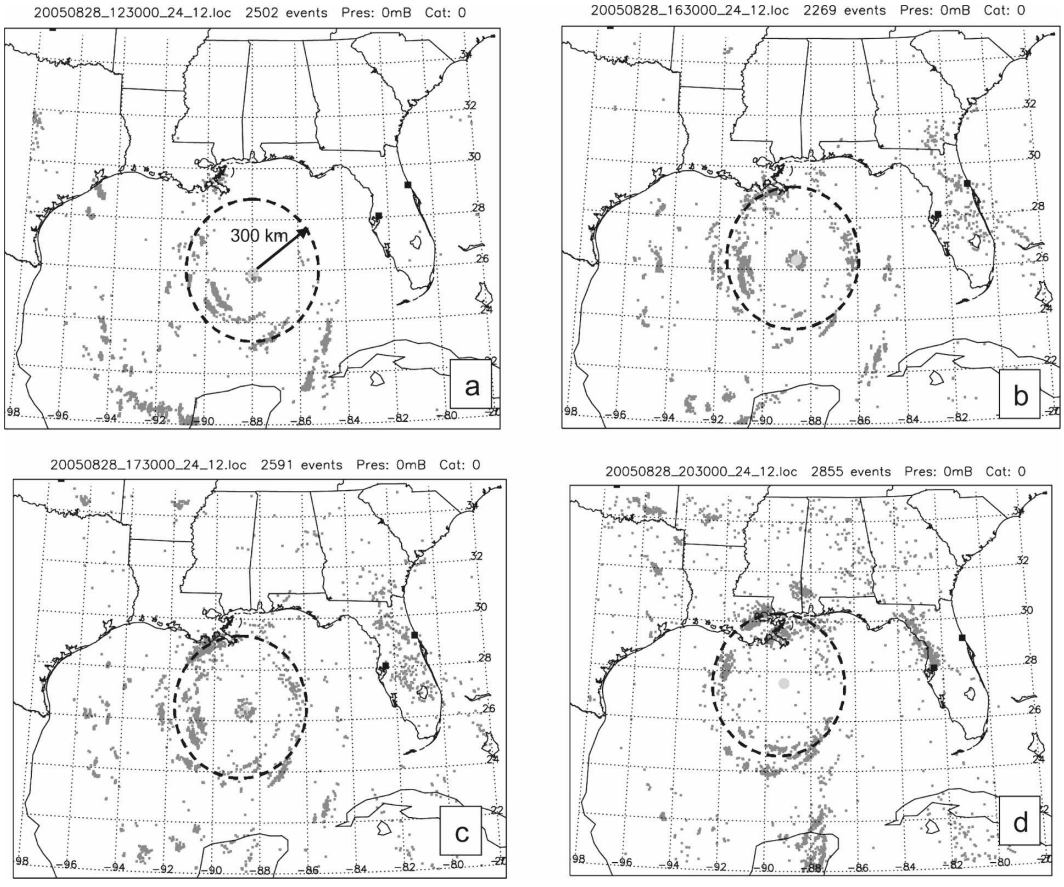

FIG. 1. Lightning in Hurricane Katrina (2005) at different times (after Shao et al. 2005). Zones of lightning are marked by dots; the TC eye is marked with a shaded circle. Dashed circles have a radius of about 300 km around the TC center. One can see the high lightning intensity (which even exceeds that over the land) within the 250–300-km radii.

cloud-to-ground (CG) flashes that occur over the water. They found three zones of distinct electrical characteristics: (i) the inner core, which contains a weak flash density maximum; (ii) the region with a well-defined flash density minimum extending 80–100 km outside this maximum; and (iii) the outer band region, which contains a strong flash density maximum within the 200–300-km-radius ring around the hurricane center. Further investigations of lightning in tropical cyclones over the Atlantic and eastern Pacific Oceans (e.g., Cecil et al. 2002; Cecil and Zipser 2002; Demetriades and Holle 2006) reinforced many findings of MMI99 with regard to the radial distribution of the flash density. An example of the lightning activity in Hurricane Katrina (2005) at several successive time instances is presented in Fig. 1, which is from the study by Shao et al. (2005). Shao et al. (2005) applied the Los Alamos Sferic Array (LASA) data that detect lightning using "very low" and "low" radio frequency (VLF/LF) signals and used time-of-arrival techniques to locate the lightning sources. The lightning is of the cloud–ground type over the water.

According to current thinking, the charging of hydrometeors in clouds takes place in a mixed-phase region at temperatures less than about −13°C when collisions of ice crystals and graupel occur in the presence of supercooled droplets (e.g., Takahashi 1978; Saunders 1993; Cecil and Zipser 2002; Sherwood et al. 2006). Therefore, a significant mass of supercooled drops must ascend in clouds above ~5–6 km to trigger flash formation. Actually, the lightning onset indicates significant changes in the cloud dynamics and in the microphysics of maritime clouds: an increase in updrafts and in ice content and the appearance of supercooled water at high levels. Numerical investigations of lightning formation in clouds can be found, for instance, in studies by Solomon and Baker (1996, 1998), Solomon et al. (2002), Mansell et al. (2002), and Mitzeva et al. (2006).

MMI99 identify the reasons for the rarity of ground flashes in the eyewall vicinity in the absence of super-

cooled water (Black and Hallett 1986, 1999). The absence of supercooled water in the eyewall makes a significant charge separation unlikely, at least according to the current theories of noninductive charge transfer between ice particles in the presence of supercooled liquid water (Saunders 1993). The lack of supercooled water in the eyewall can be attributed both to low updrafts hardly exceeding 5 m s^{-1} (Black et al. 1996; Szoke et al. 1986; Jorgensen et al. 1985) and to low aerosol concentrations, making the eyewall clouds microphysically extremely maritime. Both reasons lead to the formation of raindrops below the freezing level; these drops fall efficiently and collect the remaining droplets. Low updrafts also do not allow the suspension of graupel, which is the key ingredient for electrification. Black and Hallett (1986) suppose that supercooled water can be eliminated by the efficient seeding of eyewall clouds by ice in the rapidly rotating storm core. The eyewall lightning outbreaks (which tend to occur within relatively small time periods of several hours) are attributed by MMI99 to the replacement of the inner eyewall by a new one, which usually precedes TC intensification. Such eyewall lightning outbreaks were also observed by Demetriades and Holle (2006) in many TCs over the Northern Atlantic and the Pacific using the Long-Range Lightning Detection Network. Eyewall replacement has been recently investigated in more detail in studies by Houze et al. (2006, 2007). MMI99 attribute the well-defined minimum in lightning flash density 80–100 km outside the eyewall to lower-tropospheric downdrafts and suppressed convection.

Finally, MMI99 attribute the well-defined flash density maximum at the TC periphery to the higher instability of environmental air flows around the storm as compared to that in the eyewall. They suppose that the environmental air is convectively unstable, in keeping with Jordan's (1958, hereafter J58) mean West Indies sounding. Williams (1995), Williams and Satori (2004), and Williams et al. (2004, 2005) stressed the dominating role of atmospheric instability with regard to the land–ocean lightning flash density difference. The question arises of whether J58's sounding is sufficiently unstable to be fully responsible for the high flash density at the periphery of a TC. Emanuel (1994) argued, for instance, that the buoyancy of oceanic convection dramatically decreases with the condensate loading, so that in fact J58's sounding turns out to be close to the neutral one. MMI99 also mention that the difference in the atmospheric instability between the eyewall and the TC periphery "cannot be a complete explanation. Tropical oceanic convection often has convective available potential energy values as large as over the land (Zipser and LeMone 1980), but it does not realize as high a fraction of the pseudoadiabatic ascent rate (Jorgensen and LeMone 1989) and contains much smaller ground flash rates than over the land (see, e.g., Lucas and Orville 1996). The reason for larger flash density in outer bands remains somewhat uncertain". Note in this connection that simulations of evolution of an idealized hurricane by FL07—using a mesoscale 2-km-resolution model with a bulk parameterization scheme describing 12 distinct hydrometeor habits (Straka and Mansell 2005) and a lightning scheme (Mansell et al. 2002)—showed much more intense convection and lightning within a TC in the ~50-km-radius central convective zone than in the outer rainbands. This result was obtained under environmental conditions typical of TC formation.

In a case in which atmospheric instability was the only mechanism affecting lightning formation, one could expect an increase in the lightning frequency in zones of high sea surface temperature (SST). To check whether lightning at the TC periphery is related to the SST we present Fig. 2, showing the SST fields in the area of Hurricane Katrina calculated using the TC–ocean coupled model of the Graduate School of Oceanography of the University of Rhode Island (I. Ginis 2007, personal communication). The line in the figure denotes the TC track. The light areas indicate zones of decreased SST caused by the TC–ocean interaction (mixing and upwelling). Times correspond to those in Fig. 1. The comparison of the SST fields and the lightning frequency indicates no obvious correlation between the SST and the lightning rate. For instance, according to Fig. 1a, at 1230 UTC 28 August 2005, intense lightning takes place to the south of the Katrina center, where the SST is relatively low (Fig. 2a). At the same time, the lightning frequency is very weak to the north of the center, where the SST is maximum. The same feature can be clearly seen during the 2030–2130 UTC period (Fig. 2c): intense lightning takes place both to the south and to the north of the TC center, whereas the SST is significantly higher to the north of the TC center. In addition, there is no clear dependence of the lightning rate within the lightning ring in the south–north direction (see, e.g., Fig. 1c), whereas the SST increases northward (Fig. 2b). Note also that the characteristic scales of the SST changes are much larger than the depth of the lightning ring. Therefore, this comparison does not reveal any relationship between the variations of SST and those of lightning activity at the TC periphery. Note that we are discussing here a particular fine effect, namely, the formation of the 300-km radius lightning ring at the TC periphery. At synoptic or glob-

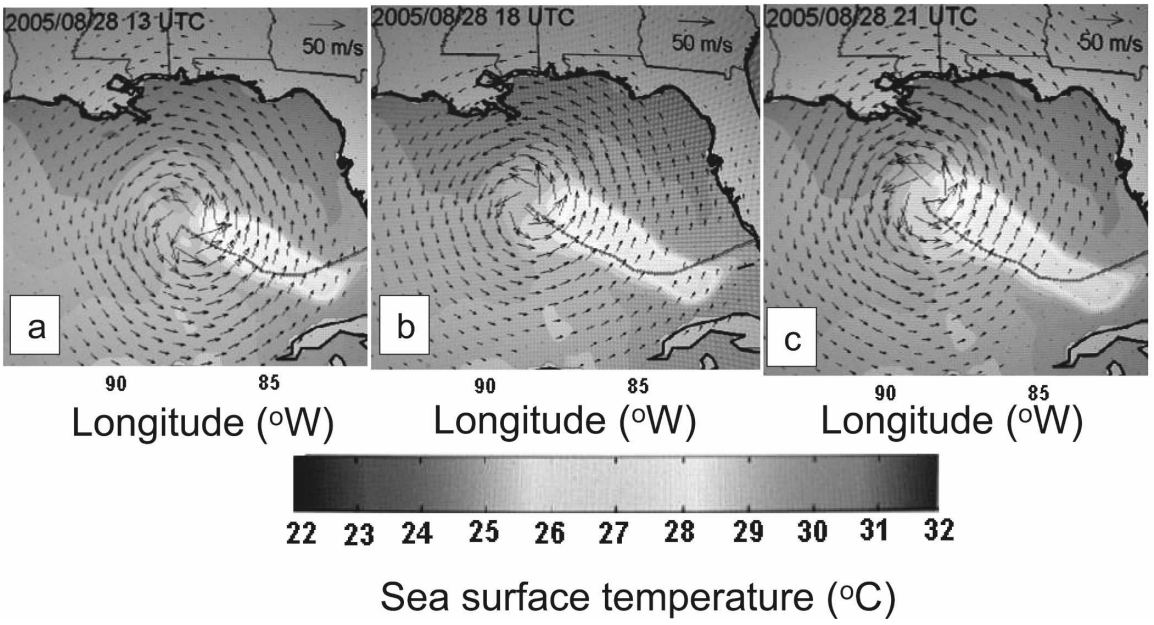

FIG. 2. SST in the area of Hurricane Katrina calculated by the TC forecast model of the Graduate School of Oceanography, University of Rhode Island (I. Ginis 2007, personal communication). The line denotes the TC track. The light areas indicate zones of the decreased SST caused by TC–ocean interaction (mixing and upwelling). Times correspond to those in Fig. 1.

al scales, a relationship between lightning and the SST indeed exists (Solomon and Baker 1998) simply because the SST fosters the development of deep convection.

Therefore, the first question we address in the paper is this: under what microphysical conditions is the instability corresponding to J58's sounding (typical of TC development; MMI99) able to provide the conditions favorable for negative ground flashes observed at the TC periphery? In a wider context, the first question can be formulated as follows: Can the high instability of the atmosphere, which can take place, say, over zones of especially high SST be considered a necessary and sufficient condition for the intense lightning formation? Going forward, numerical simulations from a high resolution cloud model with spectral bin microphysics indicate that instability is necessary, but supposedly, not sufficient for lightning formation.

In this study we check the hypothesis that continental aerosols penetrating TC clouds at the TC periphery (taken together with a higher instability at the TC periphery) create conditions favorable for lightning formation. Some support for possible aerosol effects can be found in Figs. 3a,b. Figure 3a shows that intense lightning begins when the TC approaches relatively close to the land (note that intense lightning starts on 27 August; see also Fig. 1a, corresponding to the period of the lightning ring formation). Figure 3b shows that lightning arises within the air mass downwind from the land. This air mass can contain a significant amount of aerosols, which can affect the microstructure of the convective clouds. (Note that at present it is impossible to determine the spatial structure of lightning activity in hurricanes far from the land [E. Williams and C. Price 2008, personal communication].)

The view of Hurricane Rita at 1252 EDT 23 September 2005 observed by the National Aeronautics and Space Administration's (NASA's) Tropical Rainfall Measuring Mission (TRMM) spacecraft is shown in Fig. 4. One can see that TC circulation penetrates far into the land even when the TC center is located several hundred kilometers from the coastline, which means that TCs approaching the land incoroporate a lot of continental aerosols into their circulation. This assumption will be tested using a numerical model. We will also show that these aerosols can lead to the formation of a narrow ring with a radius of 250–300 km and a high lightning flash density. Finally, we evaluate the possible effect of continental aerosols on the intensity and structure of clouds and precipitation of landfalling TC.

The effects of aerosols on individual convective clouds under conditions typical of the TC periphery are investigated using the 250-m-resolution 2D mixed-phase Hebrew University cloud model (HUCM) with spectral bin microphysics (Khain et al. 2004, 2005). The aerosol effects on the cloud structure of a TC approaching and penetrating the land are investigated using a

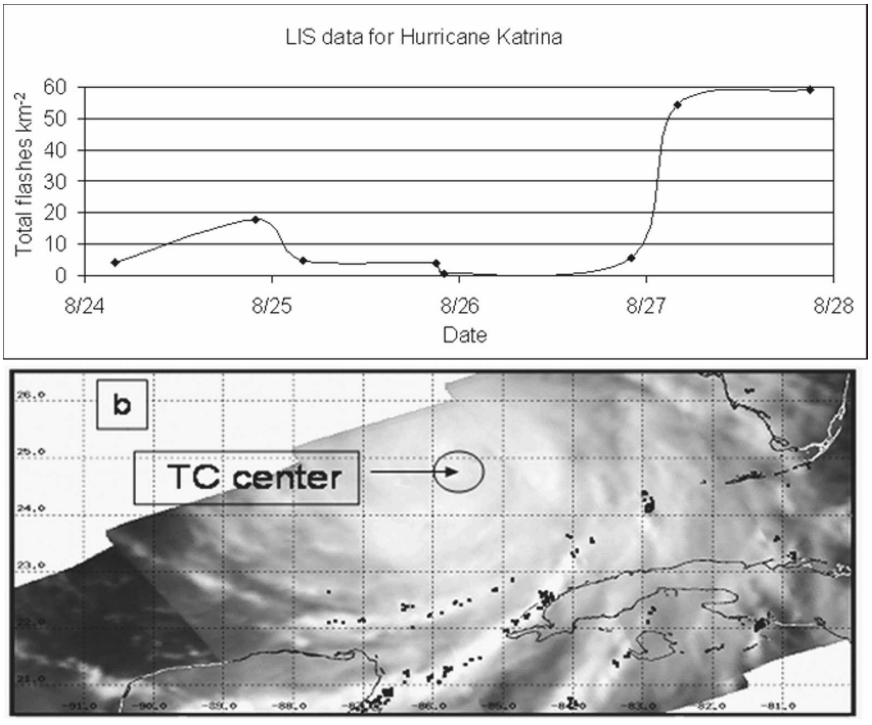

FIG. 3. (a) The time dependence of total flashes in Katrina, 24–28 Aug 2005. (b) Flash zones in Katrina (denoted by dots), 2051–2055 EDT 27 Aug. The figures are plotted using the Lightning Imaging Sensor (LIS) data. The data above indicate the total flashes for the 6° × 6° area composited to Hurricane Katrina's best-track center (http://thunder.nsstc.nasa.gov/data/#LIS_DATA).

Weather Research and Forecast (WRF; Skamarock et al. 2005) model with two nested grids. In the latter case, the WRF data were used to simulate the evolution of a TC moving along a track close to that of Hurricane Katrina from 1200 UTC 28 to 0000 UTC 30 August.

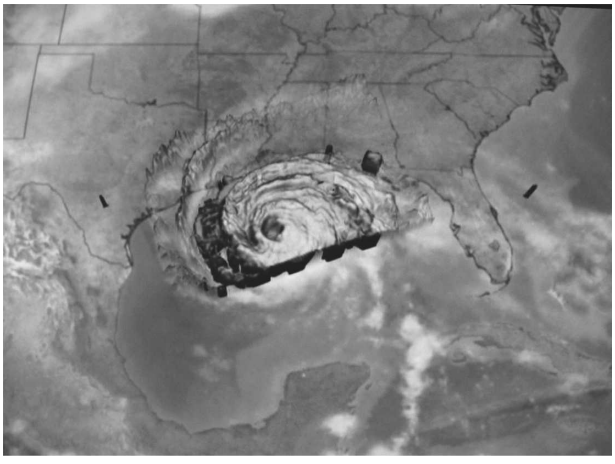

FIG. 4. Hurricane Rita at 1252 EDT 23 Sep 2005 as observed by NASA's TRMM spacecraft. The cloud cover was evaluated by TRMM's Visible and Infrared Scanner and the Geostationary Operational Environmental Satellite (GOES; http://www.nasa.gov/vision/earth/lookingatearth/h2005_rita.html).

The combination of the two models for the investigation is natural. The high-resolution HUCM can describe fine microphysical processes to evaluate the aerosol effects on the vertical profiles of liquid water and ice particles contents in individual clouds. These simulations will represent the main justification for the idea that an increase in the aerosol concentration can create conditions favorable for lightning in maritime clouds. The 3D simulations with the WRF model cannot be carried out with such high resolution and with the microphysical scheme used in the HUCM. These simulations do not resolve small clouds, and they underestimate vertical velocities. Thus, the TC simulations provide less exact but useful evidence concerning aerosol effects on individual clouds. At the same time, the 3D model illustrates the effects of aerosols on the structure of TC cloudiness and precipitation over large areas.

Taking into account the factors affecting the lightning rate (FL07), the lightning probability (LP) will be characterized by the product of the total ice content, the supercooled content, and the vertical velocity above the 5-km level.

TABLE 1. List of simulations and parameters characterizing aerosol distributions.

Type of cloud	Short title	N_0 (cm^{-3})	k	References
Maritime cloud	M	60	0.308	Khain et al. 2005
Sum of maritime and continental	M-c	2500	0.921	Khain et al. 2001b, 2004, 2005; Khain and Pokrovsky 2004
		60	0.308	
Maritime cloud with an increased fraction of large CCN	M_tail	60	0.308	Sensitivity study
		Tail: 60 CCN with radii exceeding 0.6 μm		
Sum of maritime and continental but with an increased fraction of large CCN	M_c_tail	2500 cm^{-3}	0.92	Sensitivity study
		60 cm^{-3}	0.308	
		Tail: 60 particles with radii exceeding 0.6 μm		

2. Aerosol effects on the microstructure of individual tropical maritime clouds

a. Description of the cloud model

A 2D mixed-phase Hebrew University cloud model with spectral bin microphysics has been used (Khain and Sednev 1996; Khain et al. 2004, 2005) to investigate whether an increase in aerosol concentration in the maritime tropical convection zone can change the cloud microphysical structure of individual clouds to favor lightning formation. The HUCM model microphysics is based on solving a kinetic equations system for size distribution functions for water drops, ice crystals (plate, columnar, and branch types), aggregates, graupel, and hail and/or frozen drops, as well as atmospheric aerosol particles (APs). Each size distribution is described using 43 doubling mass bins, allowing simulation of graupel and hail with sizes up to 5 cm in diameter. The model is specially designed to take into account the AP effects on the cloud microphysics, dynamics, and precipitation. The initial (at $t = 0$) cloud condensation nuclei (CCN) size distribution is calculated using the empirical dependence

$$N = N_o S_1^k \tag{1}$$

and applying the procedure described by Khain et al. (2000). In (1), N is the concentration of activated AP (nucleated droplets) at the supersaturation S_1 (in %) with respect to water, and N_o and k are the measured constants. The values of the constants used in the simulations are presented in Table 1. At $t > 0$ the prognostic equation for the size distribution of nonactivated AP is solved. Using the value of S_1 calculated at each time step, the critical AP radius is calculated according to the Kohler theory. The APs with radii exceeding the critical value are activated and new droplets are nucleated, and the corresponding bins of the CCN size distributions become empty.

The primary nucleation of each type of ice crystal is performed within its own temperature range, following Takahashi et al. (1991). The dependence of the ice nuclei concentration on supersaturation with respect to ice is described using an empirical expression suggested by Meyers et al. (1992) and applied using a semi-Lagrangian approach (Khain et al. 2000), allowing the utilization of the diagnostic relationship in the time-dependent framework. The secondary ice generation is described according to Hallett and Mossop (1974). The rate of drop freezing is described following the observations of immersion nuclei by Vali (1975, 1994), and homogeneous freezing according to Pruppacher (1995). The homogeneous freezing takes place at temperature about $-38°C$. The diffusional growth and evaporation of droplets and the deposition and sublimation of ice particles are calculated using analytical solutions for supersaturation with respect to water and ice. An efficient and accurate method of solving the stochastic kinetic equation for collisions (Bott 1998) was extended to a system of stochastic kinetic equations calculating water–ice and ice–ice collisions. The model uses height-dependent drop–drop and drop–graupel collision kernels, following Khain et al. (2001a) and Pinsky et al. (2001). Ice–ice collection rates are assumed to be temperature dependent (Pruppacher and Klett 1997). An increase in the water–water and water–ice collision kernels caused by the turbulent inertia mechanism was taken into account according to Pinsky and Khain (1998) and Pinsky et al. (2007). Advection of scalar values is performed using the positively defined conservative scheme proposed by Bott (1989). The computational domain is 178 km $\times$ 16 km with a resolution of 250 and 125 m in the horizontal and vertical directions, respectively.

b. Design of simulations with the cloud model

Simulations of individual maritime deep convective clouds under conditions typical of tropical oceans during the hurricane season (J58) have been performed. The sounding used is quite close to that observed during the 261-day Global Atmospheric Research Program (GARP) Atlantic Tropical Experiment (GATE-74) used for cloud simulations in many studies (e.g., Ferrier and Houze 1989; Khain et al. 2004, 2005). The sounding used indicates high, about 90%, humidity near the surface. The sea surface temperature is 27°C. The averaged wind shear is 15 m s^{-1} per atmospheric layer of 14-km depth. The zero temperature level is at 4.2 km. The reasons for the choice of the J58 sounding in our simulations are as follows: The J58 sounding was used by a great number of scientists to simulate TC genesis and evolution (e.g., Khain and Sutyrin 1983; Khain 1984). This sounding was mentioned by MMI99 in their attempt to explain why the lightning at the TC periphery is stronger than in the eyewall. The main reason why this sounding has been used in our 2D simulations is that it is quite unstable and leads to the formation of deep convective clouds with a vertical velocity maximum of 18–20 m s^{-1} (see below). Such vertical velocities are unusually high for maritime convection (with typical updrafts of 5–10 m s^{-1}). We used this sounding to check the "thermal" or "instability" hypothesis, namely, is atmospheric instability the sufficient condition for lightning formation? In other words, are the conditions favorable for lightning formation if vertical updrafts are high but aerosol concentration is very low?

Note that we have no data concerning the possible aerosol flux from the land to the sea area. Hence, we assume that the aerosol particle size distributions over the sea can be represented as the sum of the distributions typical of maritime and continental conditions. The aerosol particles in all simulations were assumed soluble. Under high winds, the aerosol size distribution can contain a significant amount of large cloud condensation nuclei because of sea spray formation. Hence, the penetration of continental aerosol must create aerosol size distributions containing a significant concentration of both small continental aerosols and tails of large aerosols. To investigate the effects of a high concentration of small continental aerosols on cloud microphysics and dynamics in the presence of a significant amount of large maritime CCN, the following simulations have been performed (see Table 1):

(i) The M case corresponds to the typical maritime distribution outside the area of strong winds. In this case the maximum radius of dry AP was set equal to 2 μm. The CCN number (at $S = 1\%$) was set equal to 60 cm^{-3}. The activation of the largest APs leads to the formation of 10-μm -radius droplets.

(ii) In the M_c case, the AP distribution represents the sum of a continental AP distribution (with a maximum AP radius of 0.6 μm) and the maritime distribution, similar to the M-case described previously. We suppose that this case represents the AP size distribution over the sea when continental aerosol intrusion under weak and moderate winds occurs.

(iii) In the M_tail case, the AP distribution is similar to that in the M case within the dry AP radii range below 0.6 μm, but with an AP concentration 100 times higher for radii exceeding 0.6 μm. As a result, the concentration of dry CCN (at $S = 1\%$) with the radii exceeding 0.6 μm is 60 cm^{-3}, which includes a concentration of 2-μm -radius CCN of 3.5 cm^{-3}. We suppose that this case may represent the AP distribution under hurricane winds in the central TC zone.

(iv) In the M_c_tail case, the AP is the same as in the M_c case, but with a large CCN tail of the size distribution used in the M_tail case. We suppose that this case represents the AP size distribution under the intrusion of continental aerosols and very strong wind.

The parameters N_o and k assumed in these simulations and the corresponding references are presented in Table 1. We have not included CCN with a dry radius above 2 μm in the simulations. In all simulations, clouds were triggered by an initial heating within the zone centered at $x = 54$ km to allow the cloud hydrometeors to be located in the computational zone during a longer time period. The maximum heating rate was set equal to 0.01°C s^{-1} in the center of the 4.9 km × 2 km heating area and was decreased linearly to the periphery of the zones. The duration of initial heating was 600 s in all experiments. The maximum value of the dynamical time step was 5 s. Most simulations were conducted for 3 to 4 h.

c. Results of simulations

The first important result was the following: the tail of large CCN (within a radius range of 0.6 to 2 μm) actually does not influence cloud microstructure and precipitation in the presence of a high concentration of small CCN. For instance, horizontally averaged accumulated rain amounts in the M_c and M_c_tail simulations are very similar (Fig. 5). This result can be explained as follows: The rate of the diffusion growth is determined by supersaturation. In the case when about

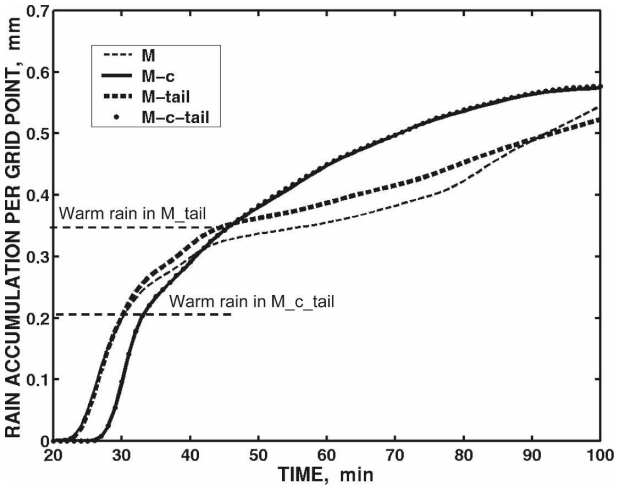

FIG. 5. Time dependence of accumulated precipitation at the surface in simulations with different concentrations and size distributions of aerosols (see Table 1). The horizontal dashed lines denote the approximate amount of warm rain in the simulations. The remaining accumulated rain is mostly cold (melted) precipitation. The warm rain from the clouds developing in the polluted air is smaller than that in the cloud developing in clean air. At the same time, the total accumulated rain is larger in clouds developing in polluted air.

1000 cm^{-3} droplets are nucleated (as in the M_c and the M_c_tail cases), the supersaturated water vapor is shared among a great number of droplets and the supersaturation is small. Moreover, the droplets growing on large CCN also contribute to the decrease in the supersaturation. As a result, the largest nucleated droplets with an initial radius of about 8 μm grow relatively slowly and reach the size necessary to collect smaller droplets at heights of ~5.5–6 km. It is necessary to recall that smaller droplets increase their size by diffusional growth faster than the largest ones (Rogers and Yau 1989), so at the 6-km level the contribution of the CCN tail to the concentration of raindrops is not substantial. A stronger effect of the large tail takes place in the case of low droplet concentration, when supersaturation is higher than in the case of high droplet concentration. Hence, raindrops in the M_tail case form at about 3 km and not at 4 km as in the M case. The accumulated rain in the M_tail run is larger than that in the M case during the first 1.5 h. However, the difference between the rain amounts is not substantial in this case either. The low sensitivity of clouds developing under tropical maritime environmental conditions to the amount of large CCN allows us to discuss the effects of continental aerosols on TC clouds under a high uncertainty regarding the concentration of large CCN. Because we expect the existence of the tail of large CCN in the TC clouds, we will discuss the effects of continental aerosols on the cloud structure in the M_tail and the M_c_tail simulations below. Note that no giant CCN with radii above 15–20 μm, which are able to trigger drop collisions immediately after their penetration into a cloud, were assumed in the simulations.

Figure 6 shows the fields of cloud water content (CWC; i.e., droplets with radii below 50 μm) in the M_tail and M_c_tail simulations at $t = 25$ min. One can see that although the CWC in clouds with a low AP concentration decreases dramatically above 3.5–4 km because of rapid raindrop formation, the CWC in clouds with a high AP concentration remains significant up to the upper atmosphere. The latter is a typical feature of clouds developing in highly polluted air (e.g., Andreae et al. 2004; Ramanathan et al. 2001; Khain et al. 2004, 2005). The specific feature of the present results is that high CWC forms in polluted air in the presence of a high concentration of large CCN. Figure 7 shows the fields of (top) crystal, (middle) graupel and (bottom) hail and/or frozen drops contents in the (left) M_tail and (right) M_c_tail simulations. One can see that these contents are higher in the clouds developing

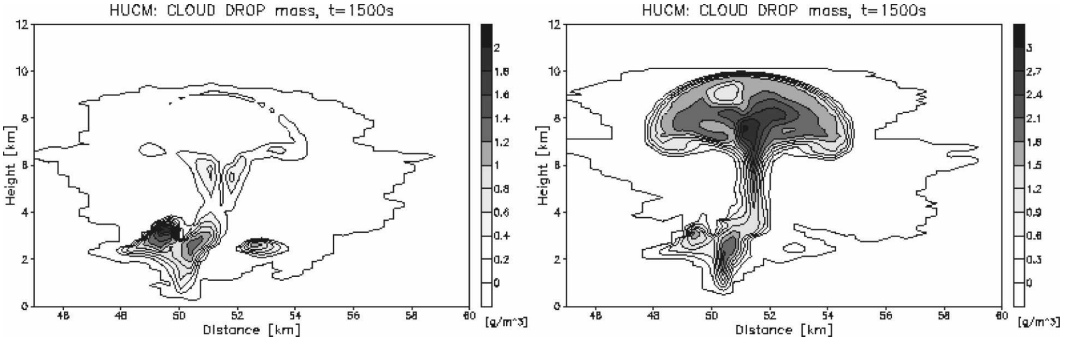

FIG. 6. CWC (droplets with radii below 50 μm) in the (left) M_tail and (right) M_c_tail simulations at $t = 25$ min. The CWC is significantly higher and reaches higher levels in the clouds developing in polluted air.

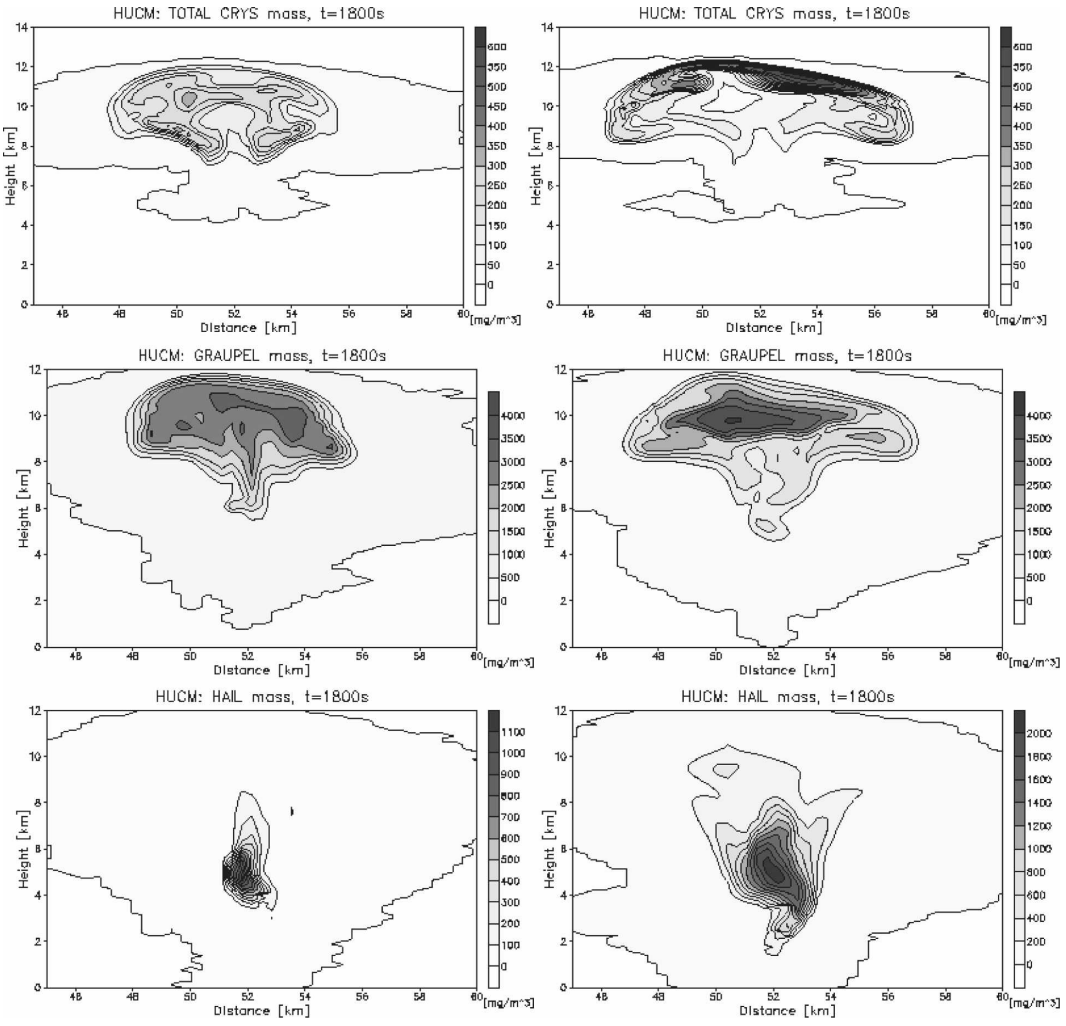

FIG. 7. (top) Crystal, (middle) graupel, and (bottom) hail/frozen drops contents in the (left) M_tail and (right) M_c_tail simulations. These contents are higher in the clouds developing under high aerosol concentrations.

in continental air, which can be attributed to a larger amount of the CWC penetrating above the freezing level in this case. On average, the total mass of graupel under high aerosol concentration is about 1.5 times higher than in cases of low aerosol concentrations. Figure 8 shows the vertical velocity in the M_tail and M_c_tail runs at $t = 25$ min. One can see that the vertical velocities in the clouds developing within high AP concentration air are higher by a few meters per second than in the clouds developing under low aerosol concentrations. This aerosol effect on cloud dynamics was simulated and discussed in detail by Khain et al. (2005) and then simulated in many studies (e.g., Lynn et al. 2005a,b; Wang 2005). The increase in the vertical updrafts in tropical clouds developing in air with microphysically continental characteristics can be attributed to an extra latent heat release caused by an extra condensational droplet growth (larger CWC) and an extra freezing (higher ice contents); see Figs. 6 and 7. Note that the difference between the vertical velocities (a few meters per second) is much smaller than the maximum updrafts of 15–18 m s^{-1}. Thus, the effect of aerosols on maximum velocities is comparatively small. The vertical velocities are determined mainly by the CAPE in agreement with the results reported by Williams (1995) and Williams et al. (2004, 2005). The cloud base tops were actually similar in both clean and polluted air cases. This result agrees well with those reported by Khain et al. (2005). The comparatively small effect of aerosols on the dynamical characteristics of clouds can be attributed as follows: On the one hand, the latent heat release in the clouds developing in the high CCN concentration case is larger, which can be seen by the generation of larger condensate mass (see Figs. 4 and

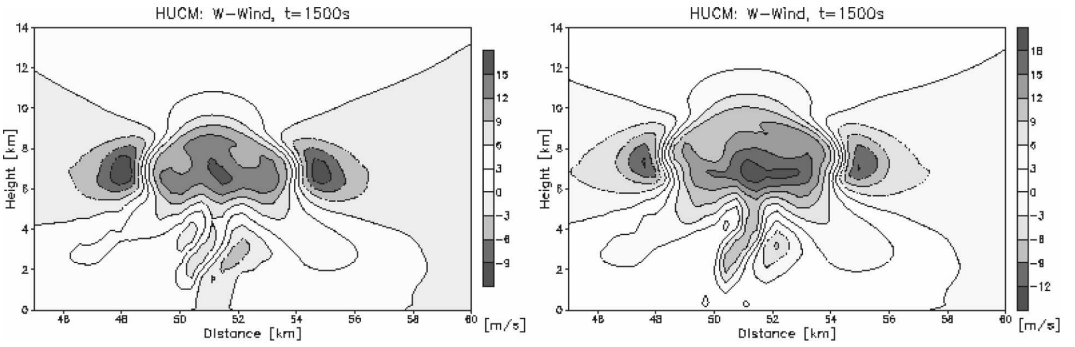

FIG. 8. Vertical velocity in the (left) M_tail and the (right) M_c_tail at $t = 25$ min. The vertical velocities in the clouds developing within the high AP concentration air are higher by several meters per second than in the clouds developing under low aerosol concentrations.

5). On the other hand, the mass loading in clouds developing in the microphysically continental air is larger. These two factors have opposite effects on the buoyancy and largely compensate for each other. Thus, the dramatic difference between the microstructure of clouds seen in Figs. 6 and 7 can be attributed mainly to aerosol effects. The comparison of the mass contents fields shown in Figs. 6 and 7 indicates that favorable conditions for the charge separation (the coexistence of a significant amount of supercooled water, ice crystals, and graupel at temperatures below −13°C) exists only in the case of high aerosol concentration. Hence, the second conclusion that can be derived from the results is that the instability of the atmosphere at the TC periphery corresponding to J58's sounding is necessary, but the condition is not sufficient to create the microphysical structure favorable for intense electrification.

Note that the problem here is even more interesting. As a matter of fact, instead of the J58 sounding, we could use an even more unstable sounding, typical, for instance, of summertime Texas (see, e.g., Khain and Pokrovsky 2004). Both the J58 sounding and the Texas sounding clouds, with a droplet concentration as low as ~50 cm^{-3}, produced heavy warm rain and a negligible amount of supercooled water at −20°C level. So it appears that aerosols represent an important component for producing a significant amount of supercooled water at the upper levels even under unstable atmospheric conditions, and in particular under maritime conditions. From the physical point of view, such situations can be explained as follows: Under both tropical and continental (like Texas) conditions, the freezing level is high (above 4 km). The vertical velocities in such clouds reach their maximum at heights of ~5–6 km (see Fig. 8). Below this level, the vertical velocities are usually smaller than the sedimentation velocity of rain drops (~9.5–10 m s^{-1}). Hence, if raindrops form below the 4–5-km level, as takes place under low aerosol concentrations, they will fall. This result is based on numerical cloud model output constrained with the aerosol distribution parameters listed in Table 1.

Figure 9 shows (top) the radar reflectivity fields in the (left) M_tail and (right) M_c_tail simulations, probably representing the clouds in the eyewall (clean air) and at the peripheral cloud bands with continental aerosol intrusion, respectively. The comparison shows that the high values of the radar reflectivity in the clouds forming in the case of high AP concentration reach (or more accurately, start at) higher levels as compared to the clouds developing in clean air. (One can expect that the air in a TC eyewall can be regarded as clear; see below). Figure 9 also shows (bottom) the rain structure of Hurricane Rita measured by the TRMM Microwave Imager (TMI) at 1252 EDT 23 September 2005. At this time the storm was a category-4 hurricane with a minimum pressure of 924 mb and sustained winds of 60 m s^{-1}. The zones with a precipitation rate of at least 2.0 inches of rain per hour (58 mm h^{-1}) are marked. One can see that the model reveals some similar features, notably that precipitation particles start forming at higher levels at the TC periphery than in the eyewall.

We interpret all these results as some justification of the hypothesis that aerosols penetrating into the maritime convective clouds are able to dramatically change cloud microphysics and dynamics. These effects plus the atmospheric instability make possible the coexistence of cloud ice and supercooled water at high levels with temperatures below −13°C—that is, the formation of thunderstorms over the ocean.

Figure 5 shows the time dependence of accumulated precipitation at the surface in the simulations with different concentrations of small and large CCN (see Table 1). Horizontal dashed lines denote the transition from the warm rain regime to the cold (melted) rain. This transition is seen by the change in the slopes of the

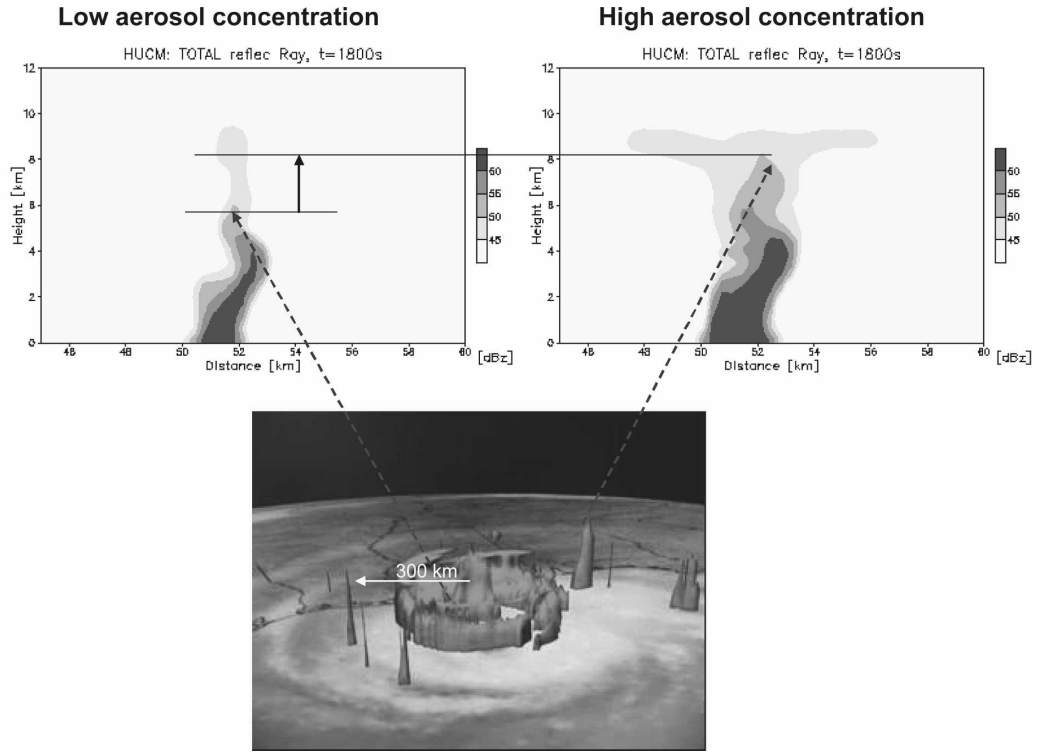

FIG. 9. (top) Radar reflectivity in the (left) M_tail and (right) M_c_tail simulations representing clouds in the eyewall and at the peripheral cloud bands with simulated continental aerosol intrusion. The radar reflectivity indicating the existence of large precipitating particles reaches higher levels in continental air. (bottom) The rain structure of Hurricane Rita measured by TMI at 1252 EDT 23 Sep 2005. At this time the storm was a category-4 hurricane with a minimum pressure of 924 mb and sustained winds of 60 m s^{-1}. Zones with rain rates exceeding 2.0 inches per hour are plotted (1252 EDT 23 Sep 2005; http:/www.nasa.gov/vision/earth/lookingatearth/h2005_rita.html).

curves. Cold (melted) rain is less intense and the slope is lower. The ratio of the accumulated rain amount toward the end of warm rain and beginning of cold (melted) rain to the total accumulated rain represents the fraction of the warm rain within the cumulative precipitation. One can see that the accumulated precipitation from clouds developing in microphysically continental air is higher, which corresponds to a higher convective heating of the atmosphere. As was discussed in Khain et al. (2004, 2005, 2008), more accumulated rain is related to the generation of larger condensate mass in clouds developing in polluted air. At the same time the precipitation loss in the wet air by evaporation is low. There was no secondary cloud formation in these simulations. In addition, the warm rain amount decreases in clouds developing in microphysically continental air, so that most precipitation in dirty clouds is cold rain formed by melting graupel and hail. On the contrary, precipitation from clouds developing in clean air is mainly warm rain.

It is reasonable to assume that the concentration of aerosols decreases from the TC periphery toward the TC center. This decrease can be caused by the washout of aerosols in TC rainbands, as well as by the significant time required by the aerosols to reach the TC center in the TC boundary layer (see below). Hence, the conditions at the TC periphery where the concentration of continental CCN is higher remain favorable for lightning formation during the whole time period during which the TCs are in the vicinity of land.

The conclusions derived in this section help us to carry out the simulations using a 3D mesoscale model.

3. Aerosol effects on the TC approaching the land: Design and results of numerical simulations

A WRF model with two nested grids was used to simulate landfall of a hurricane in the Gulf of Mexico. The resolutions of the finest and the outermost grid were 3 and 9 km, respectively. The number of the vertical levels was 31, with the distances between the levels increasing with the height. The grid structure is shown in Fig. 10. The Thompson et al. (2006) bulk parameterization scheme was applied. Hurricane Katrina (August

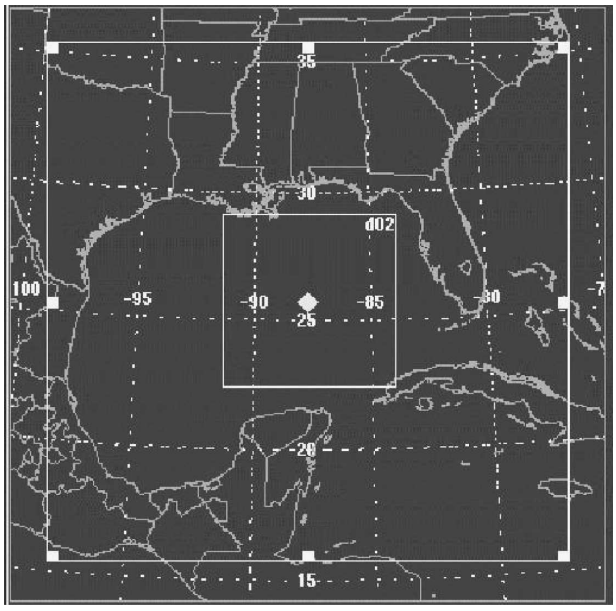

FIG. 10. The grid system structure. The location of grids corresponds to that at the beginning of the second simulation stage. The innermost grid moves with the TC center.

2005) is the TC chosen as the case study. The initial fields were taken from the Global Forecast System Reanalysis data. The lateral boundary conditions were updated every 6 h using the data as well. The Gulf of Mexico surface water temperatures were initialized at 1200 UTC 28 August and were not updated during the experiments described below.

Note that the WRF model used was not a TC forecast model, so no specific adjustment procedures were used to adapt the TC structure derived from the crude-resolution reanalysis data to the intensity of the real TC at $t = 0$. Hence, some relaxation period was required to get the model TC intensity close to the observed one. Note, however, that the accurate prediction of Katrina's intensity was not the primary purpose of the study. Hurricane Katrina has been simulated accurately in many studies using TC forecast models (e.g., Houze et al. 2006, 2007) and we were not going to compete with these studies. The main purpose of the simulations was to compare the lightning spatial distributions in the simulations with and without aerosol effects on the clouds at the TC periphery in a strong hurricane, which would be able to involve aerosols from the continent. Because of computer limitations, the simulations were performed in two stages.

At the first stage the TC was simulated from 0000 UTC 27 August (when it was located to the south of Florida) up to 0000 UTC 30 August. The purpose of the simulation was to check whether continental aerosols, which were assumed to be located initially over the land (with zero concentration over the sea), might be involved in the TC circulation and might penetrate as much as 300 km towards the TC center around the appearance of lightning in the Gulf of Mexico (Fig. 1). Aerosols were considered to be a passive scalar in the run. Figure 11 (left-hand side) shows the time dependence of the minimum pressure and the simulated tracks of the TC. The minimum pressure and track of TC Katrina are shown as well. One can see that the model TC (after some spinup period) reaches the intensity of Hurricane Katrina. The errors in the location of TC center are small and can hardly significantly affect the formation of the spatial aerosol distribution. We believe that these results indicate that the model TC creates a field of continental aerosol concentration quite similar to what could be expected around Hurricane Katrina. Figure 12 shows the field of aerosol concentration toward the end of the first stage of simulations. One can see that aerosols do penetrate the lower troposphere of the TC over time. At about 1200 UTC 28 August, aerosols form a front at a radius of about 250–300 km and a quite sharp gradient of aerosol concentration, whereas at radii $r \geq 250$ km the concentration in the lower atmosphere was actually similar to that over the land, and the central TC zone (radii < 250 km) was free of continental aerosols. These results indicate that although lightning at distances of a few hundred kilometers from the TC center may be related to aerosols, as is hypothesized in the present study, the lightning in the TC eyewall seen in Fig. 1 is not related to continental aerosol effects. Note that developed rainbands form in the TC within about a 300-km radius. We suppose that the concentric lightning ring seen in Fig. 1 forms in the zone of the aerosol "front," which transforms the maritime clouds into thunderstorms with more continental characteristics. Figure 12 (left) shows that the aerosols penetrate closer toward the TC center on the south side. This effect can be attributed to the fact that aerosols are advected along spirals by the TC wind speed. Aerosols starting their motion at the continent (to the north of the TC) should approach the TC center during their motion along the spirals because of the radial wind directed inward. Thus, aerosols should be closer to the TC center on the southern and the eastern sides of TCs than on the west side. However, the AP concentration decreases along the streamlines. Hence, the concentration on the south side turns out to be higher than on the east side. It is interesting to note that the spatial distribution of the AP concentration obtained in the simulation resembles the locations of negative ground flashes observed during the hurricane stage in nine storms in the western Atlantic (see

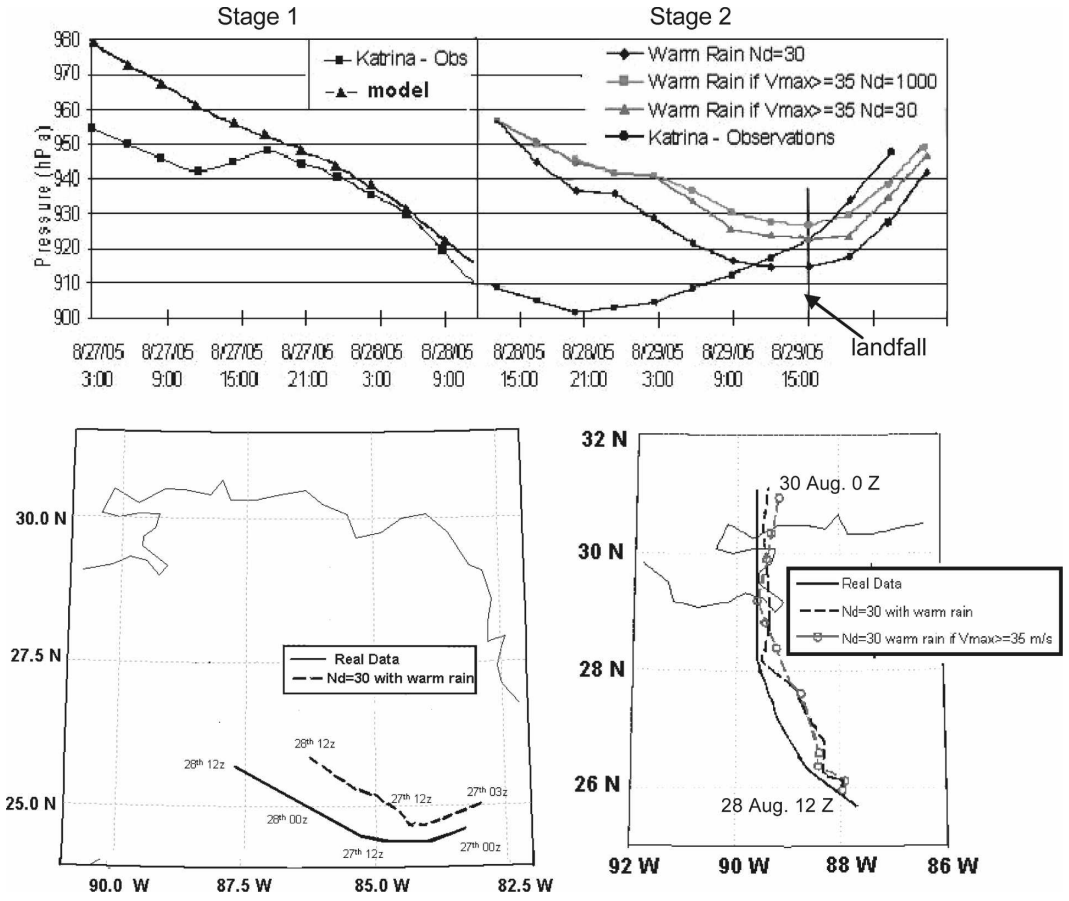

FIG. 11. Time dependencies of the minimum pressure and tracks of the model TC and of Katrina in two simulation stages: (left) 27–28 and (right) 28–29 Aug. The top left panel indicates that the modeled TC has an intensity close to that of TC Katrina. The errors in the location of the TC center are small and do not affect the spatial aerosol distribution. These results suggest that the circulation of the model TC involves aerosols from land similar to as in Katrina. The top right panel shows that the warm rain prevention at the TC periphery increases the pressure by 7–12 mb (i.e., decreases the TC intensity).

the right-hand side of Fig. 12, adapted from MMI99), composited with respect to the hourly center position of each hurricane. One can see a good correlation between the distribution of aerosols and the lightning density. The similarity of the fields may be interpreted as some evidence of the validity of the aerosol hypothesis (at least, it does not contradict the hypothesis).

In the simulation in which aerosols are treated as a passive scalar, the aerosol front approaches the TC center in the inflow layer quite slowly, with the velocity close to the radial velocity of the flow. Passive aerosols reach the central TC at about the time when Katrina was quite close to the land and the lightning in its eyewall had already terminated (Fig. 1, right-hand side). When cloud–aerosol interaction is taken into account, the concentration of continental aerosols must decrease from the TC periphery toward the TC center even more intensely because of the washout of aerosols in the TC rainbands.

The results indicate the following:

(i) The lightning in the TC eyewall is not related to aerosols involved into the TC circulation from the continent. To attain a significant concentration of supercooled droplets above the −13°C level in the TC eyewall, the vertical velocities must be especially high (or some still unknown mechanisms should be involved). At the same time, the conditions at the TC periphery where the concentration of continental CCN is high remain favorable for flash formation during the whole time period when the TC approaches or penetrates the land. This result agrees with the observations that lightning in the TC eyewall takes place only during eyewall re-

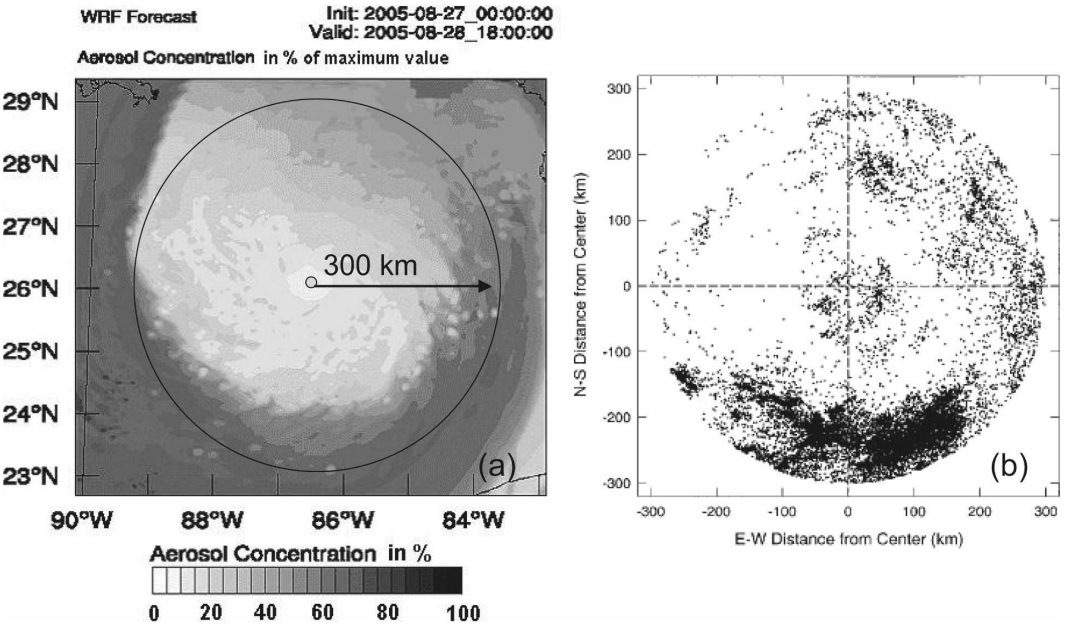

FIG. 12. (a) Aerosol concentration simulated in the lower troposphere in the TC zone at 1200 UTC 28 Aug as a percentage of the maximum value assumed to be over the continent. Aerosols form a front with a radius of ~250–300 km and penetrate closer toward the TC center on the south side. (b) As in (a), but composited with respect to the hourly center position of each hurricane (figure adapted from MMI99). One can see a good correlation between the distribution of aerosols and the lightning density.

placements, whereas the lightning is a permanent feature at the TC periphery of TCs approaching the land (see, e.g., Fig. 1).

(ii) The problem of whether giant CCN arise in the zone of the maximum winds or not is not very important for our purpose because continental aerosols do not reach the TC center (or at least not in the TC simulated in the study).

In relation to the results obtained at the first stage (aerosol transport), a question arises as to whether the transport of aerosol by the low-level wind field in the days before Katrina is able to redistribute continental and maritime aerosols in such a way as to increase aerosol concentration over the Gulf of Mexico and so affect the aerosol distribution around the TC while it approaches land. To answer the question, we performed a supplemental simulation of aerosol transport starting with 24 August 2008, when Katrina was to the east of Florida. Figure 13 shows the field of aerosol concentration (in % of the maximum value assumed over the land) toward the end of 25 August 2005. One can see that the increase of aerosol concentration over the Gulf of Mexico during the 2 days preceding the TC (24–25 August 2008) was negligible. One can also see that the TC starts involving aerosols into its circulation at earlier stage; however, the concentration or aerosols around the TC is not high at this time. Note that TC circulation also affects aerosol concentration over Florida. At the same time, aerosol concentration to the north of the Gulf of Mexico remains high and is actually equal to that of the initial concentration. We attribute

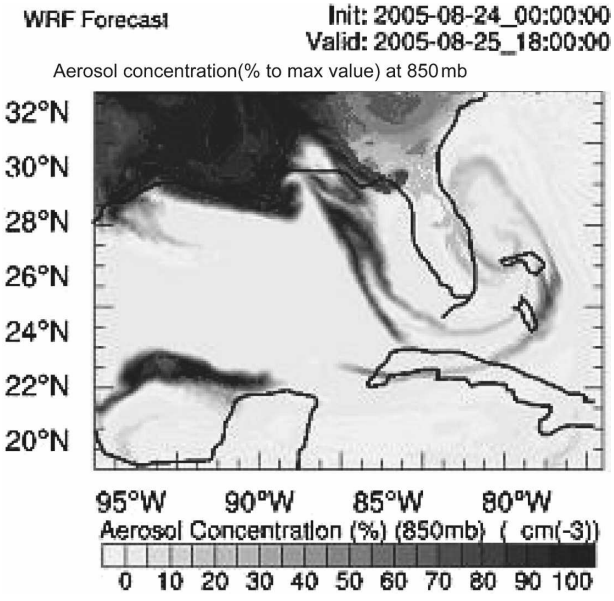

FIG. 13. Aerosol concentration simulated in a supplemental simulation in the lower troposphere at 1800 UTC 25 Aug as a percentage of the maximum value assumed to be over the continent at $t = 0$.

this result to two causes: (i) the TC circulation creates the northern winds over the land at this time and aerosols are advected from the remote areas over the land and (ii) the TC was relatively weak at this time. It starts intensifying after penetrating the Gulf of Mexico. The high concentration of aerosols remains over the land for a comparatively long period of time and starts decreasing only when TC penetrated the Gulf of Mexico. As a result, the aerosol distribution around the TC in the supplemental run was quite similar to that shown in Fig. 12. Note that in these simulations we did not take into account aerosol scavenging by clouds over the sea, which is quite effective (Rosenfeld et al. 2002). This effect should continuously decrease aerosol concentration over the sea in the absence of TCs. Furthermore, we did not take into account the generation of aerosols over land caused by anthropogenic sources. The restoration of the continental aerosol concentration was performed only via the boundary conditions, in which the aerosol concentration was assumed unchanged in the case of the air inflow. Thus, the results of the supplemental run show both that the aerosol concentration over the Gulf of Mexico remained small before the TC penetration into its area and also that some decrease in the aerosol concentration over the land (the area of Florida and northward) caused by Katrina has a small effect on the distribution of aerosols around the TC during the time of lightning triggering.

At the second stage, calculations were performed for the cases in which the aerosol effects on TC clouds were taken into account. The calculation was performed within the period 1200 UTC 28 August to 00 UTC 30 August. The way the aerosol effects were accounted for requires some preliminary comments. The 3-km resolution and the relatively crude vertical resolution do not allow one to reproduce the fine microphysical cloud features discussed in section 2c. It is well known that crude resolution decreases vertical velocities, whose values are of crucial importance for the simulation of cloud dynamics, microphysics, and precipitation. As was shown by Khain et al. (2004), the increase in the distance between the neighboring grids in the 2D HUCM from 250 m to 1 km resulted in a decrease in the maximum vertical velocities from 25 to 10 m s^{-1}. Because the fall velocities of different hydrometeors do not depend on the grid resolution, the cloud microphysical structure turns out to be quite different under different grid resolutions. For instance, the terminal velocity of raindrops is about 10 m s^{-1}. If the vertical updraft velocity is less than 10 m s^{-1}, raindrops will rapidly fall out. Thus, the utilization of the crude resolution artificially makes the clouds "maritime" by their character, even if the concentration of AP is high. Besides, most bulk parameterization schemes (at least those available in the WRF package) are, as a rule, less sensitive to aerosols than the spectral bin microphysical scheme (Lynn et al. 2005b). This statement is true with respect to the version of the Thompson et al. (2004) scheme used in the simulations (Li et al. 2008). The scheme by Thompson et al. (2004, 2006) used in the simulations was adapted from the Reisner–Thompson scheme included in MM5 (Lynn et al. 2005b). The parameterization uses the Berry and Reinhardt (1974) autoconversion scheme. The direct simulation of clouds with the bulk parameterization scheme, just by presetting different droplet concentrations at the cloud base, would most likely underestimate aerosol effects in cloud microphysics in the 3-km resolution model. To sidestep this problem, we simulated the effects of continental aerosols in the simulations by preventing warm rain in the scheme altogether. As seen in Fig. 5, it is hardly possible to prevent warm rain in maritime deep clouds by an increase in aerosol concentration up to the magnitudes typical of continental conditions. However, small aerosols significantly decrease the warm rain amount, and, even more relevantly, the prevention of warm rain in the 3D model allows the reproduction of aerosol effects qualitatively similar to those obtained in the 2D 250-m-resolution cloud model, namely, a substantial transport of large CWC upward and an increase in the ice content.

The following simulations were performed with the 3D WRF model at the second stage. The control run allowed warm rain (WR) formation by drop–drop collisions (the WR run). In this run, droplet concentration at the cloud base N_d was set equal to 30 cm^{-3}. This case corresponds to the M case with the 2D model, where CCN concentration (at $S = 1\%$) was assumed to be 60 cm^{-3} (usually about half of the available CCN are activated). In the second run, referred to as "no warm rain at the periphery" (NWRP-30), aerosol effects were parameterized by shutting off the drop–drop collisions only at the hurricane periphery, where the surface wind was smaller than 35 m s^{-1}. This threshold was chosen because the continental aerosol concentration in the TC central zone where wind speed exceeds 35 m s^{-1} should be negligibly small, as was discussed above. Besides, very high wind speed supposedly is able to produce a significant amount of giant CCN in the eyewall, which most likely renders any effects of small aerosols ineffective. Hence, warm rain is shut off only in that part of the hurricane that has winds speeds less than the threshold value. A similar approach has been used by Rosenfeld et al. (2007).

The third simulation, referred to as NWRP-1000, is similar to NWRP-30, but the droplet concentration at

the cloud base was set to 1000 cm^{-3}. This is a supplemental run, whose purpose was to illustrate the difficulties connected with simulation of the continental aerosol effects on maritime convection using the model with crude horizontal and vertical resolution and changing only the droplet concentration.

Figure 11 (bottom right) shows the tracks of the simulated storms in the WR and NWRP-30 runs (the TC track in the NWRP-1000 was actually similar to that in NWRP-30) as well as the track of Hurricane Katrina. One can see that the model reproduces Katrina's track well enough. The deviation of the model TC track from that of the real TC can be attributed to the errors in the initial TC intensity derived from the reanalysis data rather than to aerosol effects. The simulated minimum pressures of the storm with time are shown in Fig. 11 (top right). After a relatively short spinup period, the simulated TC reaches superhurricane intensity with a minimum pressure of ~915–920 hPa, also observed in Katrina. In spite of the differences between the intensity of the simulated TC and that of Karina during the spinup period, the intensity of the simulated storm was quite close to that of Katrina when the intense lightning at Katrina's periphery was observed (Fig. 1). The main result that follows from Fig. 11 and those presented below is that aerosols affecting hurricane clouds affect both TC structure and intensity. One can see that a TC with polluted air at its periphery has a smaller intensity than one in clean air throughout the entire simulation. This effect (see below) can be attributed to convection invigoration at the TC periphery caused by turning off the warm rain (representative of the potential impacts of high concentrations of aerosols on the formation of droplets). As a result, some fraction of the air moving within the inflow layer ascends at the periphery instead of reaching the TC eyewall. Hence, the rate of the latent heat release within the eyewall decreases, which results in some increase in the central pressure.

Figure 14 shows the maximum values of the supercooled CWC above 5 km in the (left) WR (with warm rain permitted) and (right) NWRP-30 simulations with no warm rain at the TC periphery. One can see a good qualitative correspondence of values obtained in the 3D simulation and those found in the 2D individual cloud simulations: the CWC maximum in microphysically continental air is about 5 g kg^{-1}, whereas in the clean air it does not exceed 2 g kg^{-1}. The amount of ice in the air with high AP concentration air is also larger than that in the clean air. For example, Fig. 15 shows the maximum total ice contents. One can see the aerosol-induced increase in the total ice content at the TC periphery in agreement with the results of the 2D model with the spectral microphysics. The maximum values of the total ice content are also in good agreement with the 2D results.

The difference between the condensate mass contents in WR and NWRP-30 indicates the differences in the latent heat release and the vertical updrafts (Fig. 16). The maximum vertical velocity in many small clouds arising in polluted air exceeds 10 m s^{-1}, whereas in the TC central zone the typical maximum vertical velocity ranges mainly from 4 to 10 m s^{-1}. One can see that aerosols increase the intensity of convection within the cloud bands located at a distance of 250–300 km from the TC center. This radius corresponds to the TC's most remote cloud bands. Figure 17 shows the vertical cross sections of the differences (NWRP30 − WR) of the azimuthally averaged fields of the total ice content $Q_{t,\mathrm{ice}}$, the cloud water content (Q_c), the rain content (Q_r), and the vertical velocity. One can see that aerosols invigorate convection and increase precipitation at a distance of about 250 km while at the same time decreasing the convection intensity between the remote rainbands and the eyewall. As a result, convection within the circle with a radius of ~250 km weakens, reducing lightning probability at a closer distance to the TC center. Note that an increase in the intensity of the rainbands at the TC periphery decreases the vertical velocity within the 50–150-km radii range. The convection within this range is suppressed (see also Fig. 15, $t = 9$ h), which leads to a decrease in the lightning probability within this radial range, in agreement with the observations of MMI99 and later studies.

As discussed above, an increase in CWC and ice content in zones of high vertical velocity should foster lightning formation. Figure 18 shows lightning probabilities, which are the maximum values of products of updrafts, the CWC, and the total ice content calculated in each grid point in a column. The two upper panels correspond to the time periods of the lightning rate depicted in Fig. 1. One can see that the LP fields calculated in NWRP-30 resemble quite well the structure of the observed lightning: the maximum lightning and LP take place within a comparatively narrow ring of the 250–300 km radius, and at the central TC zone is as a rule weaker than in the rainbands at the TC periphery. In contrast, in the WR simulation lightning is much weaker and is concentrated in the eyewall (similar to the results of FL07), which does not agree with the observations.

The lower panels of Fig. 18 correspond to the time when the entire TC has penetrated over the land and rapidly decays; they indicate that although in clean air the lightning probability decreases over land, it remains high in polluted air. Moreover, the lightning rate increases in the TC central zone. These figures show that

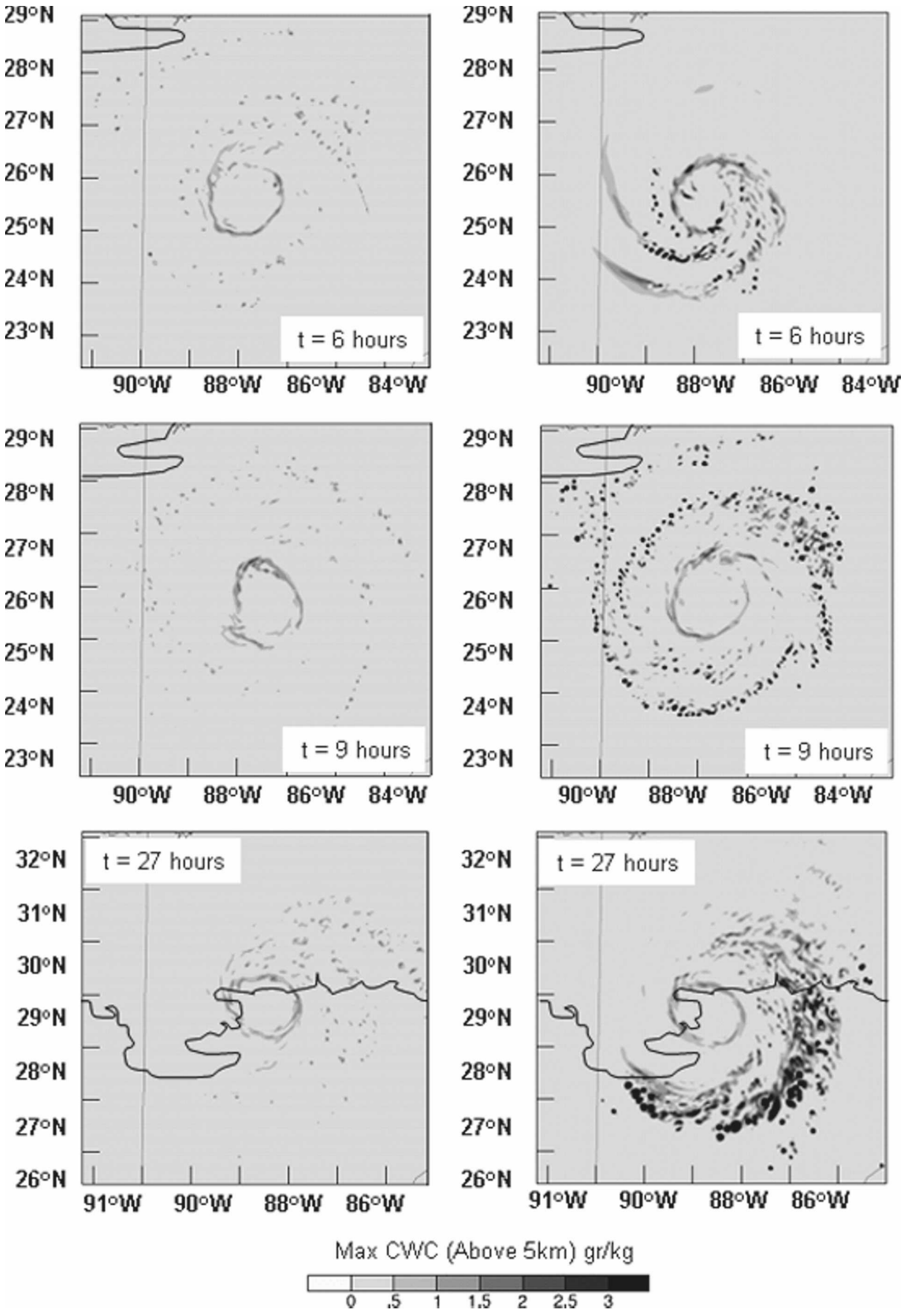

FIG. 14. Maximum values of the supercooled CWC above the 5-km level in simulations with (left) warm rain permitted and (right) no warm rain at surface wind speeds exceeding 35 m s^{-1}, for three different times.

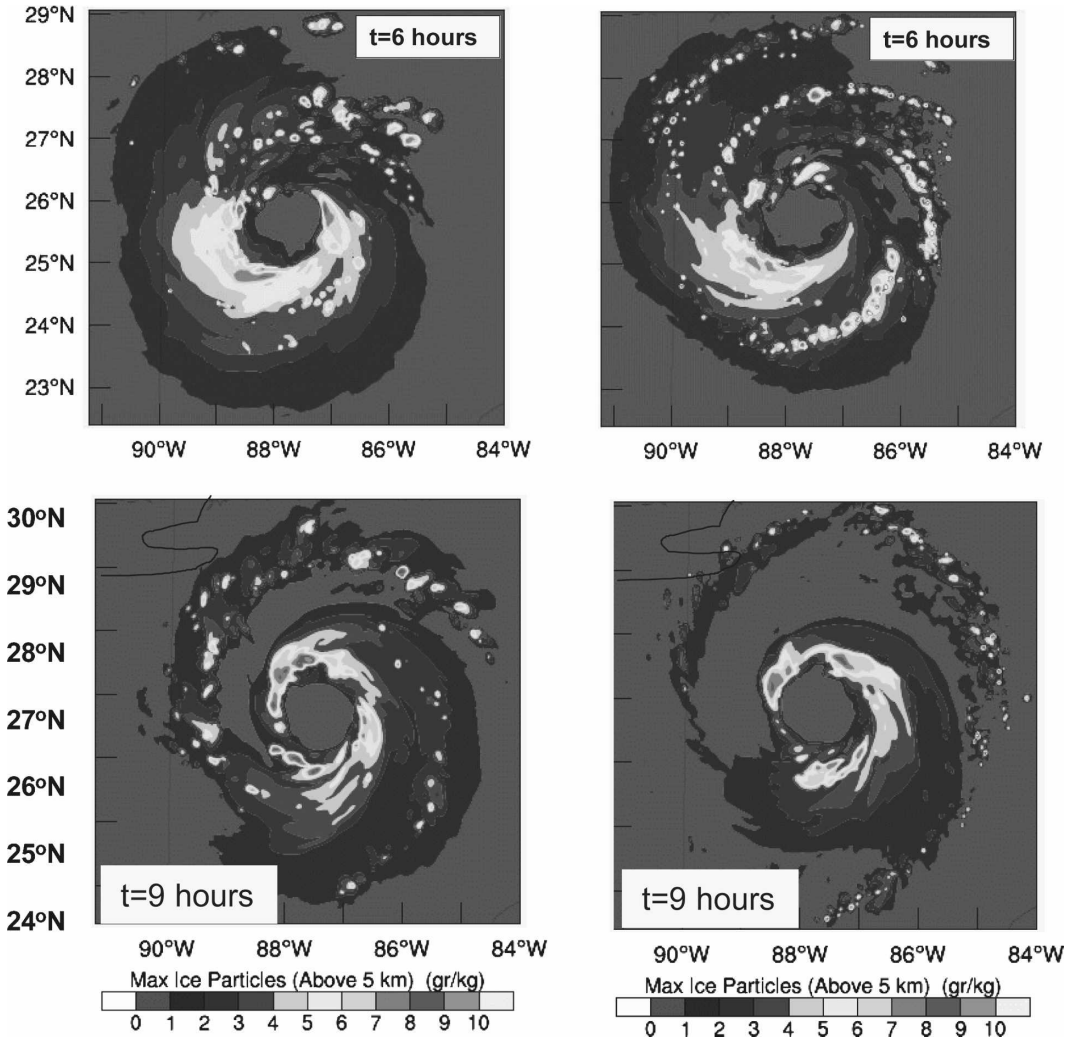

FIG. 15. Total ice content in simulations with warm rain (left) included and (right) switched off.

aerosols significantly affect the spatial distribution of intense convection in TCs.

The results also indicate that aerosols affect the cloud structure, intensity, and spatial distribution of TC precipitation approaching and penetrating the land. Figure 19 shows the precipitation rates in the simulations with warm rain allowed over the entire computational area (WR) and with warm rain has been turned off at the TC periphery (NWRP-30). One can see that when aerosol effects are taken into account, precipitation over the land increases.

Figure 20 shows the time dependences of precipitation averaged over 3-h periods within the TC zone (the internal grid) in the "warm rain" and "no warm rain" simulations. During the first 5 h, precipitation in NWRP-30 is more intense than in the WR run, presumably due to the increase of precipitation at the TC periphery. Later on, an increase in the aerosol concentration decreases precipitation within the TC zone because of the decrease in the precipitation rate in the central TC zone.

4. Discussion and conclusions

The potential effects of continental aerosols penetrating into the clouds (via the cloud bases) at the periphery of a TC approaching land on the cloud structure and the lightning rate have been investigated using a 2D cloud model with spectral bin microphysics and a 3D mesoscale WRF model with bulk microphysics. Numerical experiments with the 2D cloud model (with a resolution of 250 and 125 m in the horizontal and vertical directions, respectively) show that continental aerosols with CCN concentrations of about 1000 cm^{-3} significantly increase the amount of both supercooled cloud water and ice (mainly ice crystals, graupel, and

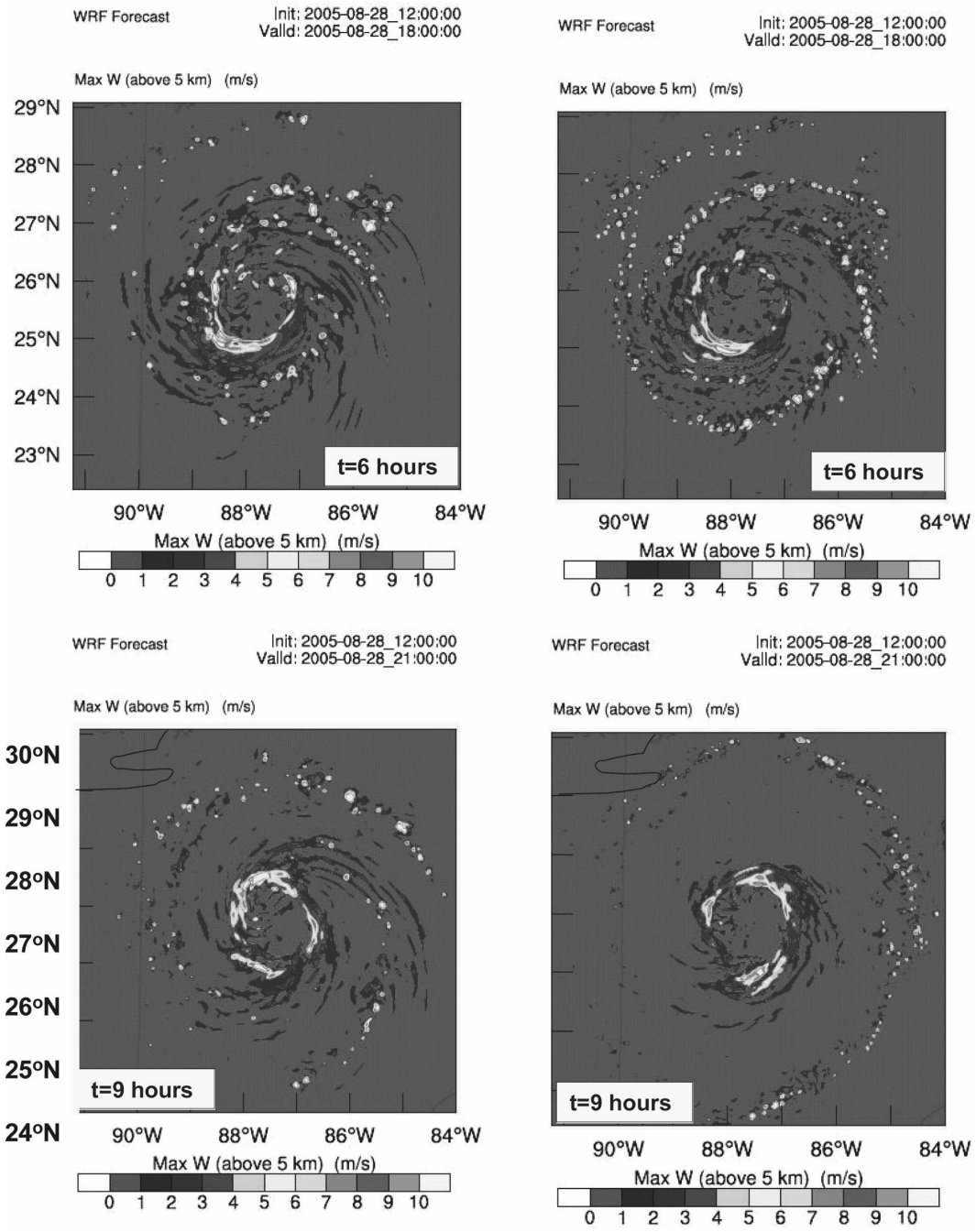

FIG. 16. As in Fig. 14, but for the vertical velocity.

hail) even under a high concentration of large CCN. In addition, the vertical updrafts were several meters per second higher in the polluted clouds. All these factors taken together lead to the coexistence of ice and cloud water within a supercooled cloud zone, which is considered to be favorable for charge separation and lightning formation.

The purpose of the simulations using a mesoscale 3-km-resolution model was to investigate the possible effects of aerosols on lightning at the periphery of hurricanes approaching the land, as well as on the cloud structure, precipitation, and TC intensity. The utilization of the 3-km resolution and crude vertical resolution, as well as the bulk parameterization scheme, do not allow one to reproduce aerosol effects related to the fine balance between the fall velocity of growing

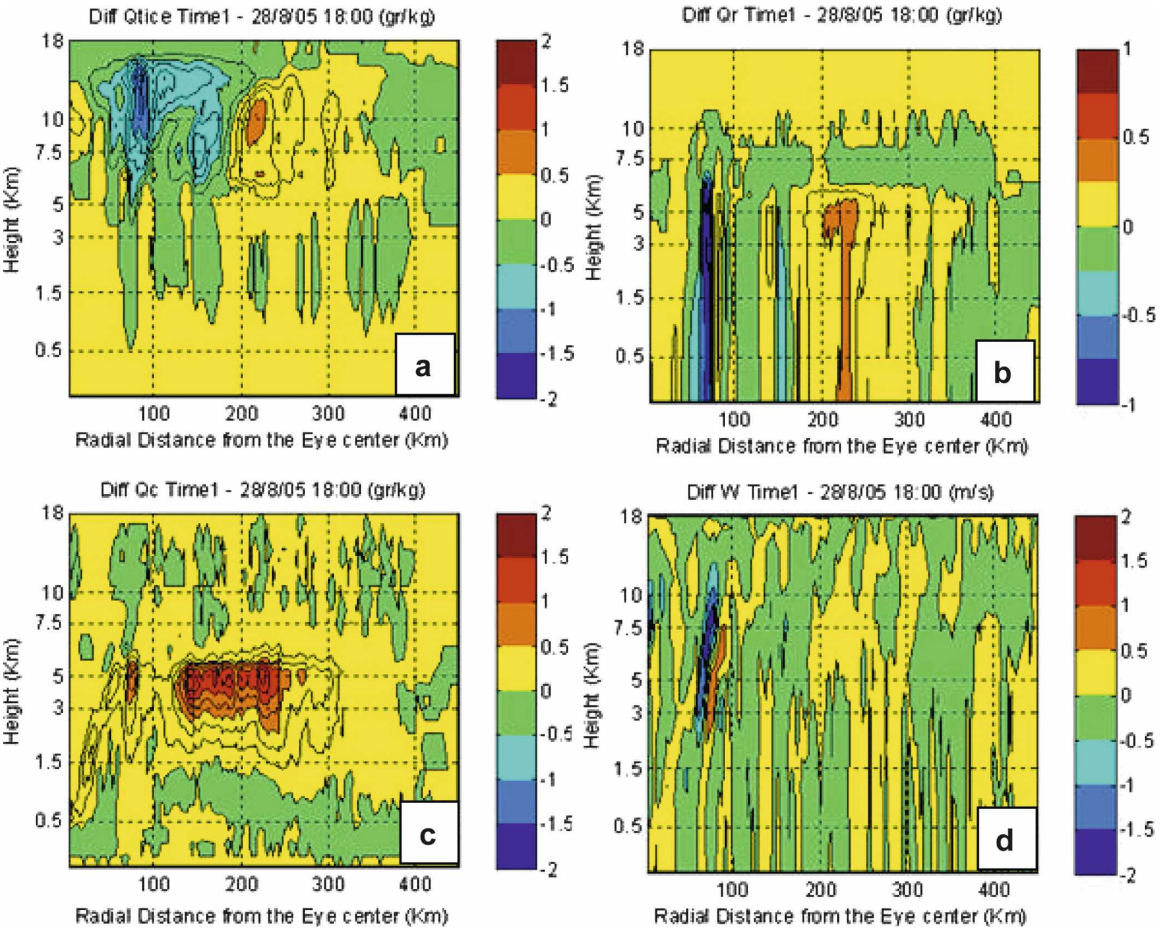

FIG. 17. Vertical cross sections of the differences (NWRP30 − WR) between the azimuthally averaged fields of (a) total ice content $Q_{t,\,\mathrm{ice}}$, (b) rain content (Q_r), (c) cloud water content (Q_c), and (d) vertical velocity. One can see that aerosols invigorate convection (and precipitation) at a distance of ~250 km (the differences are positive in the figure) while at the same time decreasing the convection intensity between the remote rainbands and the eyewall. As a result, convection within the ~200-km radius weakens, reducing lightning probability at a closer distance to the TC center.

droplets and the vertical velocity. For instance, although the results of the supplemental simulation with a droplet concentration N_d of 1000 cm^{-3} indicate some increase in central pressure and an increase in the supercooled CWC, in general the results were quite similar to those obtained in the case when the droplet concentration was set equal to 30 cm^{-3}.

As a result, the aerosol effects were parameterized by "switching off" droplet collisions and preventing warm rain at the TC periphery, where the surface wind speed was under 35 m s^{-1}. This simple parameterization of the aerosol effects leads to results that agree better with those obtained using a spectral microphysical model with a 100–250-m grid resolution.

The product of the ice content, the supercooled cloud water content, and the updraft velocity was chosen as the measure of lightning activity (lightning probability, LP). It was shown that the LP field calculated in the model resembles quite well the structure of lightning observed in that (i) the maximum lightning takes place within a comparatively narrow ring with a radius of ~250–300 km and (ii) lightning in the TC central zone is, as a rule, weaker than that in the rainbands at the TC periphery. The LP minimum was found to be related to the suppression of deep convection within the 50–150-km radius ring (see Fig. 16). This minimum becomes more pronounced when the outermost rainbands are invigorated. In the simulation, in which no aerosol effects were taken into account, the magnitude of the LP parameter was smaller and concentrated in the eyewall, which does not agree with the observations.

The analysis of the intensity variations of simulated TCs, as well as the observed variation of the intensity of Hurricanes Katrina (2005) and Rita (2005; FL07), shows that the disappearance of lightning in the TC central zone and its intensification at the TC periphery

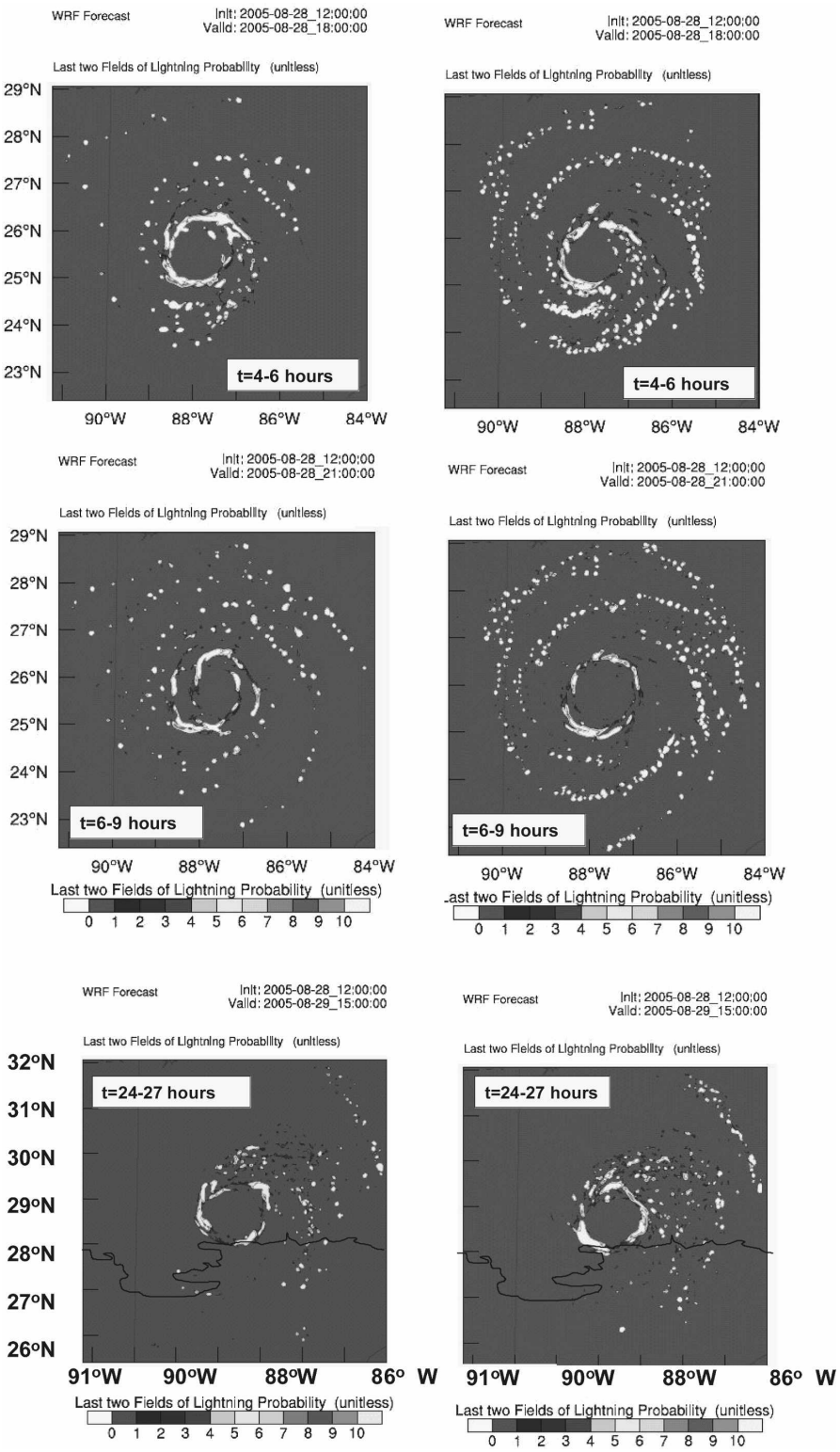

FIG. 18. Lightning probability at different times of TC evolution in the cases of clouds developing in (left) clean air and (right) continental air. The LP is calculated as the maximum product of updrafts, CWC, and total ice contents. The plotted LP represents a sum of the LP fields calculated within the time ranges shown.

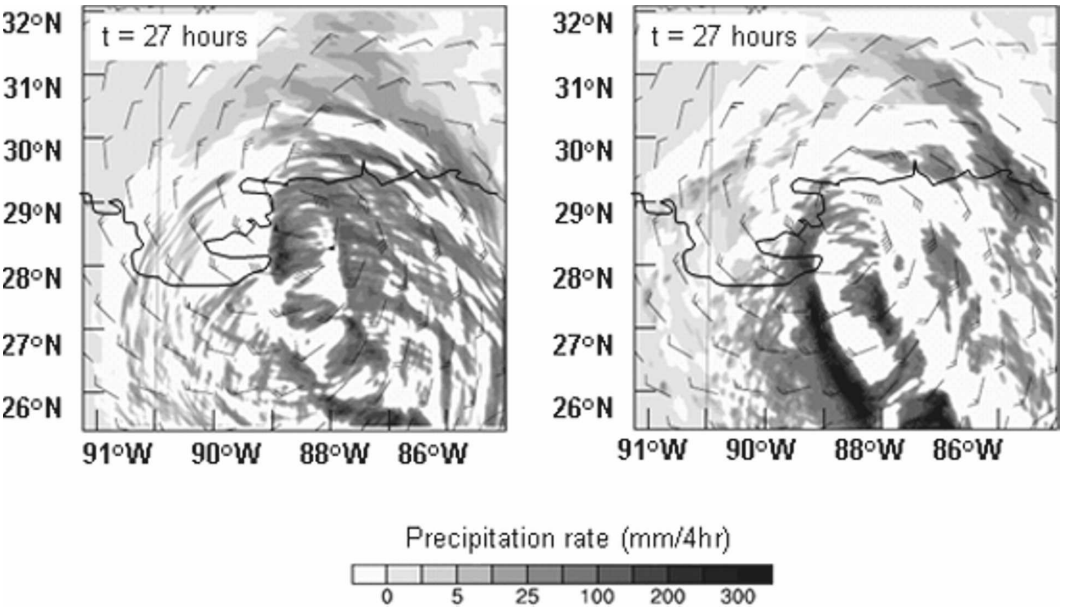

FIG. 19. Precipitation rates in the runs with (left) warm rain allowed over the entire computational area (WR) and (right) warm rain turned off at the TC periphery (NWRP-30) during TC landfall.

can be a good indicator of the TC decaying. Such behavior of TC lightning may be useful for a short-range TC intensity forecast. Note that the simulations of TC lightning in an idealized TC performed by FL07 showed negligible lightning activity at the TC periphery compared to that in the TC eyewall. The instability of the atmosphere at the TC periphery was higher than in the TC center in those simulations. However, it did not lead to convective invigoration and lightning at the TC periphery. Thus, the comment of MMI99, that the higher instability of the atmosphere at the TC periphery "cannot be a complete explanation" of the lightning maximum at the TC periphery, seems to be correct. We attribute the result obtained by FL07 to the fact that no aerosol effects have been taken into account in their simulations. Their results indicate that the changes of the instability of the atmosphere can lead to variability of the lightning in the TC eyewall, but not within a narrow ring at the TC periphery. Hence, the comparison of the results obtained by FL07 and those in this study support the assumption that lightning at the TC periphery is caused by the synergetic effect of continental aerosols and higher atmospheric instability.

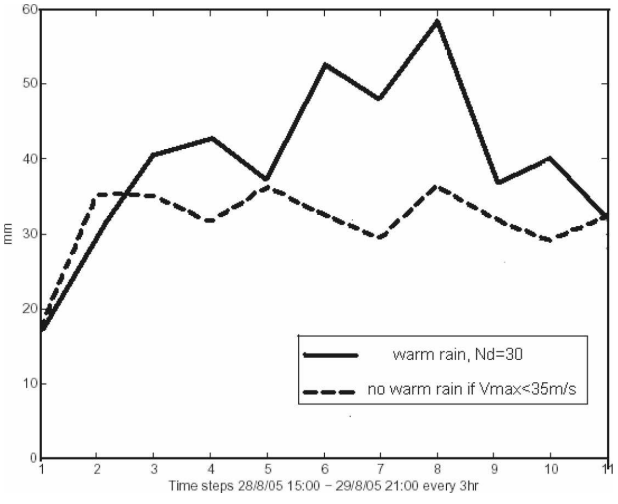

FIG. 20. Time dependences of spatially averaged 3-h accumulated precipitation within the TC zone (the internal grid) in "warm rain" and "no warm rain" (NWRP-30) simulations.

The results also indicate that aerosols affect the cloud structure, intensity, and spatial distribution of precipitation both of TCs approaching and penetrating the land and of TCs located in air of a continental nature containing a significant amount of aerosols. According to the results obtained, aerosol-induced convection invigoration at TC periphery leads to a TC weakening. From observations (e.g., Dvorak 1984) and numerical results (e.g., Khain 1984), it follows that TC formation and intensification take place when the convection is concentrated in the TC center, leading to latent heat release and falling pressure there. According to the results of a great number of simulations with a TC model (Khain 1984), the intensification of convection at TC periphery decreases the TC intensity. This decrease can be attributed to the fact that the convection invigoration at the TC periphery leads to a decrease in the air

mass penetrating to the TC eyewall and also to a decrease in the mass flux there. Correspondingly, the latent heat release also decreases in the eyewall. The second mechanism occurs as follows: Any deep cloud induces compensating downdrafts in its surroundings. As a result, deep clouds are usually surrounded by quite small ones because of the competition. This competition between clouds was studied in several studies. The convection at the TC periphery affects the convection in the TC center in the similar way. A decrease in the cloud updrafts in the TC eyewall, increase in the eyewall radius, and increase in subsidence within the central TC zone (radius of 150–200 km) caused by intensification of the convection at the TC periphery can be seen in the vertical velocity cross section in Fig. 17d.

The mechanism of the TC weakening discussed in our paper resembles the hypothesis of the field experiment Storm Fury (Simpson and Malkus 1964, Willoughby et al. 1985), according to which intensification of convection at the periphery of the eyewall should decrease air mass penetrating further toward the TC axis and weaken the wind speed maximum. However, in Storm Fury it was hypothesized that there is a significant amount of supercooled water at high levels in the eyewall. More detailed analysis (Willoughby et al. 1985) showed that there was too little supercooled water and too much ice in these clouds. Correspondingly, the cloud microphysical structure did not match the Storm Fury hypothesis. In our study, the convection invigoration is caused by small aerosols. Such invigoration agrees with both the observations (e.g., Koren et al. 2005) and the results of numerical cloud models with detailed microphysics (Khain et al. 2005, 2008). A possible application of such findings to TC mitigation by seeding is discussed by Rosenfeld et al. (2007).

Zhang et al. (2007) simulated the evolution of the idealized TC beginning with a weak initial vortex and found that the maximum TC intensity decreases when the aerosol concentration increases. No detailed physical explanation of the result was presented in that study. We suppose, however, that the reason was similar to that found in this study: Zhang et al. (2007) took aerosol scavenging into account, so the aerosol concentration was assumed to be larger at the TC periphery, as simulated in the present study.

Precipitation in the TC zone with a 350–400-km radius decreases in air with a high AP concentration mainly because of the convection weakening in the central zone of the TCs. At the same time, both the amount of precipitation at the TC periphery and the precipitation area increase. More detailed simulations are required to conclude whether continental aerosols increase or decrease precipitation from landfalling TCs over the land. We speculate that weekly variations of the anthropogenic aerosol concentration can lead to a weekly cycle of intensity and precipitation of landfalling TCs. Note that the weekly cycle of the intensity and precipitation of landfalling TCs was reported first by Cerveny and Balling (1998). They attributed the variations to the weekly variations of the anthropogenic aerosol production. According to the hypothesis by Cerveny and Balling (1998), the aerosol loading increase leads to an increase in the solar heating in the boundary layer around a cyclone. In the present study, we considered another mechanism that potentially can contribute to the weekly cycle of precipitation and the wind speed. Cerveny and Balling (1998) reported an increase in the precipitation resulting from aerosol effects. Figure 18 indicates some possibility that such increase over the land is caused by effects of aerosols on microphysical cloud structure. Note that the radiative effects of aerosols have not been taken into account in the present study. Thus, we cannot determine which mechanism is dominant. More investigations are required to make a definite conclusion.

A decrease in TC intensity under the influence of Saharan air was also reported by Dunion and Velden (2004). They attributed the decrease in intensity to thermodynamic effects. We suspect that microphysical effects of Saharan dust on TC convection may be also significant (see, e.g., Zhang et al. 2007). Further investigations are required.

According to the results obtained using the 2D cloud model, aerosols lead to a more significant increase of the CWC at higher levels than has been simulated using the WRF mesoscale model. We suppose, therefore, that the aerosol effect on the cloudiness, precipitation, and intensity of TCs may be more pronounced than that demonstrated in the study using the model with the 3-km resolution.

Note in conclusion that in spite of the encouraging and consistent results, this study must be considered to provide a plausible hypothesis as to how continental aerosols might affect hurricanes. Much more work must be done in the area of aerosol mapping and the trajectory analysis to formulate a consistent picture of TC–aerosol interactions. The utilization of high-resolution models with spectral bin microphysics is desirable to make the results quantitative. More observational studies are required to investigate the microphysical structure (e.g., supercooled water, cloud ice contents) of clouds in TCs. Observational and numerical studies are also needed to determine aerosol properties (e.g., size distributions) and aerosol fluxes from the land to tropical cyclones.

Acknowledgments. We express a deep gratitude to I. Ginis for providing results of the SST simulations in the zone of Hurricane Katrina, as well as to E. Williams and C. Price for useful observation data and advice. The study was supported by the Israel Science Foundation (Grant 140/07).

REFERENCES

Andreae, M. O., D. Rosenfeld, P. Artaxo, A. A. Costa, G. P. Frank, K. M. Longo, and M. A. F. Silva-Dias, 2004: Smoking rain clouds over the Amazon. *Science,* **303,** 1337–1342.

Berry, E., and R. L. Reinhardt, 1974: An analysis of cloud drop growth by collection: Part IV. A new parameterization. *J. Atmos. Sci.,* **31,** 2127–2135.

Black, M. L., R. W. Burpee, and F. D. Marks Jr., 1996: Vertical motion characteristics of tropical cyclones determined with airborne Doppler radar velocities. *J. Atmos. Sci.,* **53,** 1887–1909.

Black, R. A., and J. Hallett, 1986: Observations of the distribution of ice in hurricanes. *J. Atmos. Sci.,* **43,** 802–822.

——, and ——, 1999: Electrification of the hurricane. *J. Atmos. Sci.,* **56,** 2004–2028.

Bott, A., 1989: A positive definite advection scheme obtained by nonlinear renormalization of the advective fluxes. *Mon. Wea. Rev.,* **117,** 1006–1016.

——, 1998: A flux method for the numerical solution of the stochastic collection equation. *J. Atmos. Sci.,* **55,** 2284–2293.

Cecil, D. J., and E. J. Zipser, 2002: Reflectivity, ice scattering, and lightning characteristics of hurricane eyewalls and rainbands. Part II: Intercomparison of observations. *Mon. Wea. Rev.,* **130,** 785–801.

——, ——, and S. W. Nesbitt, 2002: Reflectivity, ice scattering, and lightning characteristics of hurricane eyewalls and rainbands. Part I: Quantitative description. *Mon. Wea. Rev.,* **130,** 769–784.

Cerveny, R. S., and R. C. Balling, 1998: Weekly cycles of air pollutants, precipitation and tropical cyclones in the coastal NW Atlantic region. *Nature,* **394,** 561–563.

Chronis, T., E. Williams, E. Anagnostou, and W. Petersen, 2007: African lightning: Indicator of tropical Atlantic cyclone formation. *Eos, Trans. Amer. Geophys. Union,* **88,** 40, doi:10.1029/2007EO400001.

Demetriades, N. W. S., and R. L. Holle, 2006: Long-range lightning nowcasting applications for tropical cyclones. Preprints, *Second Conf. on Meteorological Applications of Lightning Data,* Atlanta, GA, Amer. Meteor. Soc., P2.15. [Available online at http://ams.confex.com/ams/pdfpapers/99183.pdf.]

Dunion, J. P., and C. S. Velden, 2004: The impact of the Saharan air layer on Atlantic tropical cyclone activity. *Bull. Amer. Meteor. Soc.,* **85,** 353–365.

Dvorak, V. F., 1984: Tropical cyclone intensity analysis using satellite data. NOAA Tech. Rep. NESDIS 11, 47 pp.

Emanuel, K. A., 1994. *Atmospheric Convection.* Oxford University Press, 580 pp.

Ferrier, B. S., and R. A. Houze Jr., 1989: One-dimensional time-dependent modeling of GATE cumulonimbus convection. *J. Atmos. Sci.,* **46,** 330–352.

Fierro, A. O., L. Leslie, E. Mansell, J. Straka, D. MacGorman, and C. Ziegler, 2007: A high-resolution simulation of microphysics and electrification in an idealized hurricane-like vortex. *Meteor. Atmos. Phys.,* **98,** 13–33, doi:10.1007/s00703-006-0237-0.

Hallett, J., and S. C. Mossop, 1974: Production of secondary ice crystals during the riming process. *Nature,* **249,** 26–28.

Houze, R. A., Jr., and Coauthors, 2006: The Hurricane Rainband and Intensity Change Experiment: Observations and modeling of Hurricanes Katrina, Ophelia, and Rita. *Bull. Amer. Meteor. Soc.,* **87,** 1503–1521.

——, S. S. Chen, B. F. Smull, W.-C. Lee, and M. M. Bell, 2007: Hurricane intensity and eyewall replacement. *Science,* **315,** 1235–1239.

Jordan, C. L., 1958: Mean soundings for the West Indies area. *J. Meteor.,* **15,** 91–97.

Jorgensen, D. P., and M. A. LeMone, 1989: Vertical velocity characteristics of oceanic convection. *J. Atmos. Sci.,* **46,** 621–640.

——, E. J. Zipser, and M. A. LeMone, 1985: Vertical motions in intense hurricanes. *J. Atmos. Sci.,* **42,** 839–856.

Khain, A. P., 1984: *Mathematical Modeling of Tropical Cyclones.* Gidrometeoizdat, 247 pp.

——, and G. G. Sutyrin, 1983: *Tropical Cyclones and Their Interaction with the Ocean.* Gidrometeoizdat, 241 pp.

——, and I. Sednev, 1996: Simulation of precipitation formation in the Eastern Mediterranean coastal zone using a spectral microphysics cloud ensemble model. *Atmos. Res.,* **43,** 77–110.

——, and A. Pokrovsky, 2004: Simulations of effects of atmospheric aerosols on deep convective clouds using a spectral microphysics mixed-phase cumulus cloud model. Part II: Sensitivity study. *J. Atmos. Sci.,* **61,** 2983–3001.

——, M. Ovtchinnikov, M. Pinsky, A. Pokrovsky, and H. Krugliak, 2000: Notes on the state-of-the-art numerical modeling of cloud microphysics. *Atmos. Res.,* **55,** 159–224.

——, M. B. Pinsky, M. Shapiro, and A. Pokrovsky, 2001a: Collision rate of small graupel and water drops. *J. Atmos. Sci.,* **58,** 2571–2595.

——, D. Rosenfeld, and A. Pokrovsky, 2001b: Simulation of deep convective clouds with sustained supercooled liquid water down to −37.5°C using a spectral microphysics model. *Geophys. Res. Lett.,* **28,** 3887–3890.

——, A. Pokrovsky, M. Pinsky, A. Seifert, and V. Phillips, 2004: Simulations of effects of atmospheric aerosols on deep convective clouds using a spectral microphysics mixed-phase cumulus cloud model. Part I: Model description and possible applications. *J. Atmos. Sci.,* **61,** 2963–2982.

——, D. Rosenfeld, and A. Pokrovsky, 2005: Aerosol impact on the dynamics and microphysics of convective clouds. *Quart. J. Roy. Meteor. Soc.,* **131,** 2639–2663.

——, N. BenMoshe, and A. Pokrovsky, 2008: Factors determining the impact of aerosols on surface precipitation from clouds: An attempt at classification. *J. Atmos. Sci.,* **65,** 1721–1748.

Koren, I., Y. J. Kaufman, D. Rosenfeld, L. A. Remer, and Y. Rudich, 2005: Aerosol invigoration and restructuring of Atlantic convective clouds. *Geophys. Res. Lett.,* **32,** L14828, doi:10.1029/2005GL023187.

Lhermitte, R. M., and P. Krehbiel, 1979: Doppler radar and radio observations of thunderstorms. *IEEE Trans. Geosci. Electron.,* **17,** 162–171.

Li, G., Y. Wang, and R. Zhang, 2008: Implementation of a two-moment bulk microphysics scheme to the WRF model to investigate aerosol-cloud interaction. *J. Geophys. Res.,* **113,** D15211, doi:10.1029/2007JD009361.

Lucas, C., and R. E. Orville, 1996: TOGA COARE: Oceanic lightning. *Mon. Wea. Rev.,* **124,** 2077–2082.

Lynn, B., A. Khain, J. Dudhia, D. Rosenfeld, A. Pokrovsky, and A. Seifert, 2005a: Spectral (bin) microphysics coupled with a mesoscale model (MM5). Part I. Model description and first results. *Mon. Wea. Rev.,* **133,** 44–58.

——, ——, ——, ——, ——, and ——, 2005b: Spectral (bin) microphysics coupled with a mesoscale model (MM5). Part II: Simulation of a CaPE rain event with a squall line. *Mon. Wea. Rev.,* **133,** 59–71.

Mansell, E. R., D. R. MacGorman, C. L. Ziegler, and J. M. Straka, 2002: Simulated three-dimensional branched lightning in a numerical thunderstorm model. *J. Geophys. Res.,* **107,** 4075, doi:10.1029/2000JD000244.

McFarquhar, G., and R. A. Black, 2004: Observations of particle size and phase in tropical cyclones: Implications for mesoscale modeling of microphysical processes. *J. Atmos. Sci.,* **61,** 422–439.

Meyers, M. P., P. J. DeMott, and W. R. Cotton, 1992: New primary ice-nucleation parameterizations in an explicit cloud model. *J. Appl. Meteor.,* **31,** 708–721.

Mitzeva, R. P., J. Latham, and S. Petrova, 2006: A comparative modeling study of the early electrical development of maritime and continental thunderstorms. *Atmos. Res.,* **82,** 26–36, doi:10.1016/j.atmosres.2005.01.006.

Molinari, J., P. K. Moore, V. P. Idone, R. W. Henderson, and A. B. Saljoughy, 1994: Cloud-to-ground lightning in Hurricane Andrew. *J. Geophys. Res.,* **99,** 16 665–16 676.

——, ——, and ——, 1999: Convective structure of hurricanes as revealed by lightning locations. *Mon. Wea. Rev.,* **127,** 520–534.

Orville, R. E., and J. M. Coyne, 1999: Cloud-to-ground lightning in tropical cyclones (1986–1996). Preprints, *23rd Conf. on Hurricanes and Tropical Meteorology,* Dallas, TX, Amer. Meteor. Soc., 194.

Pinsky, M., and A. P. Khain, 1998: Some effects of cloud turbulence on water–ice and ice–ice collisions. *Atmos. Res.,* **47,** 69–86.

——, ——, and M. Shapiro, 2001: Collision efficiency of drops in a wide range of Reynolds numbers: Effects of pressure on spectrum evolution. *J. Atmos. Sci.,* **58,** 742–764.

——, ——, and ——, 2007: Collisions of cloud droplets in a turbulent flow. Part IV: Droplet hydrodynamic interaction. *J. Atmos. Sci.,* **64,** 2462–2482.

Pruppacher, H. R., 1995: A new look at homogeneous ice nucleation in supercooled water drops. *J. Atmos. Sci.,* **52,** 1924–1933.

——, and J. D. Klett, 1997: *Microphysics of Clouds and Precipitation.* 2nd ed. Oxford University Press, 963 pp.

Ramanathan, V., P. J. Crutzen, J. T. Kiehl, and D. Rosenfeld, 2001: Aerosols, climate, and the hydrological cycle. *Science,* **294,** 2119–2124.

Rodgers, E., J. Weinman, H. Pierce, and W. Olson, 2000: Tropical cyclone lightning distribution and its relationship to convection and intensity change. Preprints, *24th Conf. on Hurricanes and Tropical Meteorology,* Ft. Lauderdale, FL, Amer. Meteor. Soc., 537–541.

Rogers, R. R., and M. K. Yau, 1989: *A Short Course of Cloud Physics*. 3rd ed. Pergamon, 293 pp.

Rosenfeld, D., R. Lahav, A. Khain, and M. Pinsky, 2002: The role of sea spray in cleaning air pollution over ocean via cloud processes. *Science,* **297,** 1667–1670.

——, A. Khain, B. Lynn, and W. L. Woodley, 2007: Simulation of hurricane response to suppression of warm rain by sub-micron aerosols. *Atmos. Chem. Phys. Discuss,* **7,** 5647–5674.

Saunders, C. P. R., 1993: A review of thunderstorm electrification processes. *J. Appl. Meteor.,* **32,** 642–655.

Shao, X. M., and Coauthors, 2005: Katrina and Rita were lit up with lightning. *Eos, Trans. Amer. Geophys. Union,* **86** (42), 398–399.

Sherwood, S. C., V. Phillips, and J. S. Wettlaufer, 2006: Small ice crystals and the climatology of lightning. *Geophys. Res. Lett.,* **33,** L05804, doi:10.1029/2005GL025242.

Simpson, R. H., and J. S. Malkus, 1964: Experiments in hurricane modification. *Sci. Amer.,* **211,** 27–37.

Skamarock, W. C., J. B. Klemp, J. Dudhia, D. O. Gill, D. M. Barker, W. Wang, and J. G. Powers, 2005: A description of the Advanced Research WRF version 2. NCAR Tech. Note NCAR/TN-468+STR, 88 pp.

Solomon, R., and M. B. Baker, 1996: A one-dimensional lightning parameterization. *J. Geophys. Res.,* **101,** 14 983–14 990.

——, and ——, 1998: Lightning flash rate and type in convective storms. *J. Geophys. Res.,* **103** (D12), 14 041–14 057.

——, C. Adamo, and M. Baker, 2002: A lightning initiation mechanism: Application to a thunderstorm electrification model. *C. R. Phys.,* **3,** 1325–1333.

Straka, J. M., and E. R. Mansell, 2005: A bulk microphysics parameterization with multiple ice precipitation categories. *J. Appl. Meteor.,* **44,** 445–466.

Szoke, E. J., E. J. Zipser, and D. P. Jorgensen, 1986: A radar study of convective cells in mesoscale systems in GATE. Part 1: Vertical profile statistics and comparison with hurricanes. *J. Atmos. Sci.,* **43,** 182–197.

Takahashi, T., 1978: Riming electrification as a charge generation mechanism in thunderstorms. *J. Atmos. Sci.,* **35,** 1536–1548.

——, T. Endoh, G. Wakahama, and N. Fukuta, 1991: Vapor diffusional growth of free-falling snow crystals between −3° and −23°C. *J. Meteor. Soc. Japan,* **69,** 15–30.

Thompson, G., R. M. Rasmussen, and K. Manning, 2004: Explicit forecasts of winter precipitation using an improved bulk microphysics scheme. Part I: Description and sensitivity analysis. *Mon. Wea. Rev.,* **132,** 519–542.

——, P. R. Field, W. D. Hall, and R. Rasmussen, 2006: A new bulk microphysical parameterization for WRF (& MM5). *Proc. Seventh WRF Users' Workshop,* Boulder, CO, NCAR, 1–11. [Available online at http://www.mmm.ucar.edu/wrf/users/workshops/WS2006/abstracts/Session05/5_3_Thompson.pdf.].

Vali, G., 1975: Remarks on the mechanism of atmospheric ice nucleation. *Proc. Eighth Int. Conf. on Nucleation,* Leningrad, Russia, Gidrometeoizdat, 265–269.

——, 1994: Freezing rate due to heterogeneous nucleation. *J. Atmos. Sci.,* **51,** 1843–1856.

Wang, C., 2005: A modeling study of the response of tropical deep convection to the increase of cloud condensational nuclei concentration: 1. Dynamics and microphysics. *J. Geophys. Res.,* **110,** D21211, doi:10.1029/2004JD005720.

Wiens, K. C., S. A. Rutledge, and S. A. Tessendorf, 2005: The 29 June 2000 supercell observed during STEPS. Part II: Lightning and charge structure. *J. Atmos. Sci.,* **62,** 4151–4177.

Williams, E., 1995: Meteorological aspects of thunderstorms. *Handbook of Atmospheric Electrodynamics,* H. Volland, Ed., CRC Press, 27–60.

——, and G. Satori, 2004: Lightning, thermodynamic and hydro-

logical comparison of the two tropical continental chimneys. *J. Atmos. Solar-Terr. Phys.,* **66,** 1213–1231.

——, T. Chan, and D. Boccippio, 2004: Islands as miniature continents: Another look at the land–ocean lightning contrast. *J. Geophys. Res.,* **109,** D16206, doi:10.1029/2003JD003833.

——, V. Mushtak, D. Rosenfeld, S. Goodman, and D. Boccippio, 2005: Thermodynamic conditions favorable to superlative thunderstorm updraft, mixed phase microphysics, and lightning flash rate. *Atmos. Res.,* **76,** 288–306.

Willoughby, H. E., D. P. Jorgensen, R. A. Black, and S. L. Rosenthal, 1985: Project STORMFURY: A scientific chronicle 1962–1983. *Bull. Amer. Meteor. Soc.,* **66,** 505–514.

Zhang, H., G. M. McFarquhar, S. M. Saleeby, and W. R. Cotton, 2007: Impacts of Saharan dust as CCN on the evolution of an idealized tropical cyclone. *Geophys. Res. Lett.,* **34,** L14812, doi:10.1029/2007GL029876.

Zipser, E. J., and M. A. LeMone, 1980: Cumulonimbus vertical velocity events in GATE. Part II: Synthesis and model core structure. *J. Atmos. Sci.,* **37,** 2458–2469.